SCISPACE
formerly Typeset

Open access • Report • DOI:10.2172/4287064

Preparation of lanthanide oxide microspheres by sol--gel methods.

— Source link

C.J. Hardy, S.R. Buxton, M.H. Lloyd

Published on: 01 Jan 1967

Topics: Lanthanide, Oxide and Sol-gel

Related papers:

- New A/sup III/B/sup III/O$sub 3$ interlanthanide perovskite compounds
- A study of trivalent-pentavalent oxide systems
- Preparation of thin films of rare Earth oxides and investigation of their physical properties

Share this paper:

View more about this paper here: https://typeset.io/papers/preparation-of-lanthanide-oxide-microspheres-by-sol-gel-2kjt1c3o06

MASTER

ORNL-4000
UC-25 – Metals, Ceramics, and Materials

PREPARATION OF LANTHANIDE OXIDE MICROSPHERES BY SOL-GEL METHODS

C. J. Hardy
S. R. Buxton
M. H. Lloyd

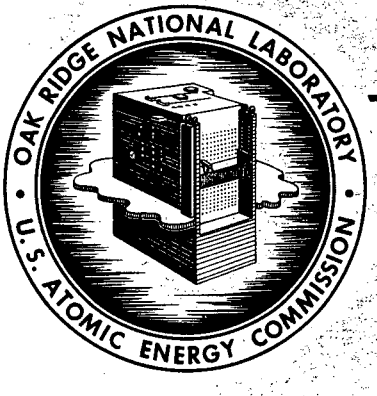

OAK RIDGE NATIONAL LABORATORY
operated by
UNION CARBIDE CORPORATION
for the
U.S. ATOMIC ENERGY COMMISSION

DISCLAIMER

This report was prepared as an account of work sponsored by an agency of the United States Government. Neither the United States Government nor any agency Thereof, nor any of their employees, makes any warranty, express or implied, or assumes any legal liability or responsibility for the accuracy, completeness, or usefulness of any information, apparatus, product, or process disclosed, or represents that its use would not infringe privately owned rights. Reference herein to any specific commercial product, process, or service by trade name, trademark, manufacturer, or otherwise does not necessarily constitute or imply its endorsement, recommendation, or favoring by the United States Government or any agency thereof. The views and opinions of authors expressed herein do not necessarily state or reflect those of the United States Government or any agency thereof.

DISCLAIMER

Portions of this document may be illegible in electronic image products. Images are produced from the best available original document.

Printed in the United States of America. Available from Clearinghouse for Federal Scientific and Technical Information, National Bureau of Standards, U.S. Department of Commerce, Springfield, Virginia 22151.
Price: Printed Copy $3.00; Microfiche $0.65

LEGAL NOTICE

This report was prepared as an account of Government sponsored work. Neither the United States, nor the Commission, nor any person acting on behalf of the Commission:

A. Makes any warranty or representation, expressed or implied, with respect to the accuracy, completeness, or usefulness of the information contained in this report, or that the use of any information, apparatus, method, or process disclosed in this report may not infringe privately owned rights; or

B. Assumes any liabilities with respect to the use of, or for damages resulting from the use of any information, apparatus, method, or process disclosed in this report.

As used in the above, "person acting on behalf of the Commission" includes any employee or contractor of the Commission, or employee of such contractor, to the extent that such employee or contractor of the Commission, or employee of such contractor prepares, disseminates, or provides access to, any information pursuant to his employment or contract with the Commission, or his employment with such contractor.

ORNL-4000

Contract No. W-7405-eng-26

OFFICIAL PRICES

H.C. $3.00; MN,65

CHEMICAL TECHNOLOGY DIVISION

PREPARATION OF LANTHANIDE OXIDE MICROSPHERES BY SOL-GEL METHODS

C. J. Hardy,* S. R. Buxton, and M. H. Lloyd

*Guest Scientist from the Atomic Energy Research Establishment, Harwell, England.

AUGUST 1967

OAK RIDGE NATIONAL LABORATORY
Oak Ridge, Tennessee
operated by
UNION CARBIDE CORPORATION
for the
U.S. ATOMIC ENERGY COMMISSION

CONTENTS

PREPARATION OF LANTHANIDE OXIDE MICROSPHERES BY SOL-GEL METHODS

C. J. Hardy, S. R. Buxton, and M. H. Lloyd

ABSTRACT

Lanthanide oxide microspheres have been produced with a controlled size in the diameter range 50 to 500 μ, a density of up to 98% of the theoretical crystal density, a low surface area (0.01 to 0.1 m^2/g), and a high resistance to crushing (up to 3 kg for 500-μ-diam spheres). Hydroxide sols and gels were used as intermediates, and the resulting spheres were calcined at a relatively low final temperature (1000 to 1500°C), which depended on the crystal form required.

Sols were prepared by precipitating the lanthanide hydroxides from lanthanide nitrate solutions with ammonium hydroxide, washing the precipitates thoroughly, and heating them for 1 hr at 80°C. These sols were concentrated by evaporation until they were 2 to 3 M in the metal ion and contained 0.06 to 0.25 mole of residual nitrate per mole of metal ion; then they were formed into gel microspheres of controlled size by partial dehydration with a long-chain alcohol in a tapered column. The gel spheres were dried further in vacuum at 120°C, heated to 500°C in vacuum to decompose the residual nitrate, and finally calcined to oxide microspheres at 1000 to 1500°C in air.

Spectroscopic methods were used to rapidly determine the nitrate and metal ion concentrations in the sols, to study the form of bonding of the components (e.g., nitrate) of the sols and gels, and to estimate the sizes of the aggregates of colloidal particles. Electron microscopy and electron diffraction measurements showed that the initial precipitates of lanthanide hydroxides consisted of amorphous particles of 30 to 60 A in diameter. When aged in the mother liquor, these particles changed into crystalline sheets up to several hundred angstroms in width; when thoroughly washed and aged in water, they changed into rods, tubes, or rolled sheets up to several thousand angstroms in length. Randomly arranged bundles of these rod-shaped crystals were present in microspheres of the lanthanide hydroxide gels. Electron micrographs of replicas of etched polished surfaces of the dense oxides obtained by heating the gels to 1450°C showed 5- to 10-μ-wide grains that contained oriented crystalline units that were 0.2 to 0.5 μ wide. These units were probably polycrystalline because x-ray line-broadening measurements indicated a crystallite size of 500 to 700 A.

Lanthanide oxides in this form have potential industrial value; for example, europium oxide in cermets could be incorporated in reactor control rods, and europium, promethium, and thulium oxides might be used in radioactive heat sources. The method of preparation is also applicable to the production of sols, gels, and oxides of the transplutonium elements, of which americium and curium are of interest for incorporation in targets for the High Flux Isotope Reactor at Oak Ridge to produce transcurium isotopes.

1. INTRODUCTION

Methods for the production and characterization of sols and gels of compounds of the lanthanide elements have been developed to obtain lanthanide oxide microspheres with densities nearly equal to the theoretical crystal density and with high resistances to crushing. The knowledge gained will be applied to the preparation of americium and curium oxides that are suitable for incorporation in targets for the High Flux Isotope Reactor (HFIR). Lanthanide oxides in this form have potential applications in industry, particularly in the nuclear field. For example, oxides of samarium, gadolinium, and europium might be used in control rods and as burnable poisons in fuel elements.

The bulk of the work in this report was concerned with the laboratory-scale preparation of sols and gels of lanthanide hydroxides that were precipitated from lanthanide nitrate solutions. The sols were subsequently formed into gel microspheres, which were calcined to dense oxide microspheres under conditions which depended on the crystal form required. The methods described are being extended to the preparation of sols and gels of a wide range of lanthanide hydroxides. They are also being scaled up to give up to 50-g batches of selected oxides (e.g., monoclinic europium oxide) to provide material for study by other investigators.

Spectroscopic methods were used (1) to rapidly determine the concentrations of nitrate and metal ion in the sols; (2) to detect differences between preparations of sols and gels that had different appearances under the microscope; (3) to study the form of bonding of the components of the sols and gels (e.g., the bonding between the residual nitrate groups and the metal ions before and during calcination to oxide); and (4) to estimate the sizes of the aggregates of colloidal particles in the sols.

Electron microscopy of the sols and gels has provided a better understanding of the various stages in the process. Results on aging of lanthanide hydroxides are in agreement with published data of Milligan and Dwight.[1]

2. PREPARATION AND PROPERTIES OF SOLS

Two principal methods were used to prepare the sols: (1) addition of an excess of NH_4OH or tetramethylammonium hydroxide (TMAH) to a solution of a lanthanide nitrate (Sect. 2.1), and (2) addition of a solution of a lanthanide nitrate to an excess of NH_4OH (Sect. 2.2). The second method is now preferred. We also tried a few other methods such as the removal of nitrate from solution with a long-chain organic amine and slow hydrolysis in homogeneous solution; these are described briefly in Sect. 2.3. The properties of the sols, with particular reference to spectra, are discussed in Sect. 2.4.

The minimum purity of the lanthanide nitrates or oxides used was 99.0% except for the europium and samarium nitrates, which had a minimum purity of 99.9%. All these compounds were obtained from the American Potash and Chemical Corporation (Lindsay Division), except for holmium oxide (99.9%), cerous nitrate, and erbium oxide (99.9%), which were

obtained from Semi-Elements, Inc., Saxonburg, Pennsylvania, the G. F. Smith Chemical Company, and Kleber Laboratories, Inc., respectively.

2.1. First Method – Addition of NH_4OH or TMAH to Lanthanide Nitrate Solution

2.1.1. Method of Preparation

Sols of lanthanide hydroxides were prepared by the following steps:

(1) The hydroxide was precipitated from a 0.1 to 0.2 M lanthanide nitrate solution by the addition of a 100% excess over the stoichiometric amount of 1 to 2 M NH_4OH or 1 M TMAH (the latter was purified from carbonate with barium hydroxide solution)* at either 0 or 25°C.
(2) The precipitate was thoroughly washed six to eight times with CO_2-free distilled water. After each wash, the precipitate was centrifuged from solution (sometimes base was added to the first two washes to decrease the amount of residual nitrate ion in the product.
(3) The precipitate was suspended in CO_2-free distilled water containing about 0.05 to 0.2 mole of nitric acid per mole of metal added and was evaporated, with stirring, at 50 to 60°C for several hours until a metal concentration of about 2 M was reached.

Microspheres of gel were formed both in beakers and in a tapered column by dehydrating the sols with a long-chain alcohol (see Sect. 4). The following conditions were necessary for the formation of microspheres that were characterized by good sphericity and a smooth surface and that could be calcined to strong microspheres of dense oxide:

(1) operation in an argon-filled glove box to minimize the absorption of CO_2;
(2) use of TMAH rather than NH_4OH (see Sect. 2.1.2);
(3) washing of the precipitate with TMAH prior to the water washes to obtain a low residual nitrate content;
(4) precipitation and washing at 0°C, rather than at 25°C, to decrease the effects of aging of the precipitate;
(5) addition of enough nitrate, in the case of Pr and Eu, to provide nitrate:metal ratios of 0.05 to 0.1 and 0.1 to 0.2, respectively, to stabilize the sol after washing steps; and
(6) evaporation to dehydrate and concentrate the initially bulky hydroxide precipitate to a metal concentration of about 2 M.

---

*Great difficulty was experienced in obtaining CO_2-free TMAH; the material, which was obtained from Eastman Kodak Co. in sealed bottles, contained about 20% as TMA carbonate. The purification method (suggested by R. G. Haire) included precipitation of the carbonate as barium carbonate by addition of a stoichiometric amount of barium hydroxide solution, and the removal of the solid by filtration in vacuum.

2.1.2. Comparison of the Use of NH_4OH and TMAH in the Preparation of Europium Hydroxide Sols

Since it was soon recognized that TMAH gave better products than NH_4OH with respect to lower residual nitrate content and a higher resistance to crushing, a comparison was made of europium hydroxide sols, gels, and oxides that were prepared by these two reagents under similar conditions. The following procedure was used: A 100% excess of each base was added to a 0.2 M solution of europium nitrate at 0°C. The resulting precipitates were washed six times with water at 0°C and centrifuged after each wash at 6000 rpm in a high-speed centrifuge. All operations were conducted in an argon atmosphere.

X-ray measurements were made on the washed precipitates, which had been protected from absorption of CO_2. The powder patterns contained broad lines that corresponded to those published[2] for $Eu(OH)_3$ and $EuO{\cdot}OH$, rather than for Eu_2O_3 [later electron diffraction measurements indicated the main component to be $Eu(OH)_3$]. The crystallite sizes calculated from the line-broadening were about 75 and 110 A for hydroxides prepared with TMAH and with NH_4OH respectively. The loss of europium hydroxide by peptization in the wash water was excessive (22%) with NH_4OH but was only slight (3.5%) with TMAH. The sols were next formed into gel microspheres and then calcined to oxide (see Sects. 4-6). The microspheres prepared with sol from the TMAH method resisted a crushing force of 300 g (mean of ten 166-μ-diam spheres), while those prepared with sol from the NH_4OH method resisted a crushing force of 150 g.

In summary, TMAH has the advantages of giving lower losses and a better oxide product but has the disadvantage of a much higher cost (equivalent to about $350 per kg of Eu_2O_3 produced). It also requires a barium hydroxide step to remove the carbonate impurity. The NH_4OH method (Sect. 2.2) is now preferred.

2.1.3. Stability and Particle Size of Praseodymium Hydroxide Sols as Functions of Nitrate Content and Temperature

Praseodymium hydroxide was precipitated from a solution of praseodymium nitrate with TMAH, and the thoroughly washed precipitate was dispersed in water to give a Pr concentration of about 0.2 M. The sol was stirred for 30 min at 25°C and then divided into two portions. Nitric acid was added to each to give NO_3^-:Pr ratios of 0.05 and 0.10, respectively, and the two sols were restirred for 1 hr at 25°C. Samples of each sol were removed to allow measurement of the absorption spectra from 7000 to 3000 A, the refractive indexes (with a Zeiss dipping refractometer), and the concentrations of metal and nitrate in a 1 M $HClO_4$ solution (see Sect. 2.4). The two sols were then heated at 70°C for 1 hr, and again samples were removed for measuring the spectra and determining the concentrations of metal and nitrate. Spectra were also measured for samples diluted (with water) to a concentration that was one-fifth that of the original.

Samples of the sol before and after heating at 70°C were aged 24 hr at 25°C. The percentage of the Pr that had sedimented by gravity was determined by spectrophotometric analysis of the supernates and the

residues, which were dissolved in perchloric acid. The following table shows the results:

NO_3^-/Pr Mole Ratio	Settling Time (hr)	Temperature (°C)	Percentage of Pr Sedimented
0.05	25	25	42
0.05	1	25	14
	1	70	
	24	25	
0.10	24	25	8
0.10	1	25	12
	1	70	
	24	25	

The apparent molecular weights and diameters of the sol particles, which were calculated from the absorption spectra of the sols at 4000 A by the method described in Sect. 2.4, are:

NO_3^-/Pr Mole Ratio	Aging		Dilution Ratio	Molecular Weight	Diameter of Assumed Sphere (A)
	Time (hr)	Temperature (°C)			
0.05	2	25	-	1.85×10^7	230
0.05	2	25	5	7.5×10^7	364
0.05	25	25	-	1.61×10^7	218
0.05	25	25	5	1.11×10^8	416
0.05	25	25	5	6.4×10^7	346
	1	70			
0.10	2	25	-	1.91×10^7	230
0.10	40	25	5	4.3×10^7	304
0.10	1	70	5	5.7×10^7	332
	40	25			

The overall conclusions are:

(1) The sol with an NO_3^-/Pr ratio of 0.1 was more stable toward sedimentation than that with an NO_3^-/Pr ratio of 0.05.
(2) Dilution of the 0.1 to 0.2 M Pr sols (with water) to a concentration that was one-fifth that of the original led to aggregation of the particles by factors of 4 to 7 and 2.3 for NO_3^-/Pr ratios of 0.05 and 0.1 respectively.
(3) Heating the sols for 1 hr at 70°C did not have a marked effect on the molecular weight.

2.2. Second Method – Addition of Lanthanide Nitrate Solution to NH_4OH

2.2.1. Method of Preparation

The steps in this method were:

(1) The hydroxide was precipitated by adding a 0.2 M lanthanide nitrate solution to a 20-fold (occasionally a 40-fold) excess of 8 M NH_4OH that was constantly being stirred in a beaker at 25°C.

(2) The precipitate was centrifuged and washed with CO_2-free distilled water five or six times, with intermediate centrifugation and decantation of the wash liquors; a volume of about 200 ml of water per gram of metal was used, and the pH of the wash liquor decreased from 11 to about 9 (Table 1);

(3) The precipitate was then a damp paste, and for La, Ce, Pr, and Nd, this paste liquefied spontaneously to form a translucent sol after aging 25°C for a period of 20 to 60 min. The hydroxide pastes of Sm, Eu, Gd, Ho, and Er did not liquefy spontaneously, and required shaking or agitation in a vortex mixer for several minutes.

After step (3), the sols had a metal concentration of 0.5 to 0.6 M when the centrifugation was done in a small, high-speed (6000-rpm) centrifuge, or 0.4 to 0.5 M when a large preparative (1100-rpm) centrifuge was used. The mole ratio of residual nitrate to metal was in the range 0.06 to 0.25; and the apparent pH (measured with a standard pH meter) was about 7.1 to 7.3 for sols that liquefied spontaneously, and 9.6 to 10.2 for those which did not. The time required to prepare 10 g of the sol was only about 1 hr. A summary of the preparative details and analyses for a range of sols is given in Tables 2 and 3.

The variation of the apparent pH of the sol with time was studied in detail for a Pr sol (No. 123) (Fig. 1). The pH of both the wash liquor and the sol decreased sharply with time until about 2 hr after the precipitation; at the same time, the viscosity of the sol also decreased markedly. For example, the viscosity of a 0.5 M Nd sol (No. 122) decreased from greater than 100 centipoises (thixotropic) to 1.7 centipoises (not thixotropic) over a time interval from 3 hr 10 min to 3 hr 40 min after precipitation, while the pH decreased from 10.1 to 7.2. The apparent pH of europium hydroxide sols remained in the region of 9.6 to 10.1 for many days at 25°C.

When a viscous Eu sol (No. 124) was heated for 1 hr at 80°C, the pH decreased from 9.8 to 6.6 and the viscosity decreased from greater than 100 to about 1.5 centipoises. The sol could then be concentrated to 2.5 M in europium hydroxide without an appreciable increase in viscosity, whereas without this heat treatment a dilute, viscous sol such as No. 124 cannot be evaporated conveniently because it sets solid. The heat-treatment step was, therefore, essential to obtain a low-viscosity sol with a metal concentration of 2 to 2.5 M, which was most suitable for forming microspheres characterized by good sphericity and surface gloss (for details of Nd, Sm, and Eu sols, see Table 4). However, the structure of the particles in the sols of europium hydroxide (and the related viscosity) had an effect on the strength of the final calcined oxide spheres (see Sect. 6.1).

Table 1. Variation of pH of Wash Liquor with Number of Washes for Lanthanide Hydroxides

Sol No.	Metal	Type of Centrifuge[a]	Apparent pH							Final NO_3^-/Metal Mole Ratio
			Initial Supernate	Wash No. 1	2	3	4	5	6	
95	Pr	HS	-	10.70	10.20	9.75	9.50	-	-	0.19
96	Eu	HS	-	10.80	10.35	9.90	9.55	-	-	-
104	Nd	LS	10.80	10.50	10.40	10.22	9.82	9.65	9.16	0.29
105	Pr	LS	-	10.70	10.45	10.15	9.90	9.40	-	0.24
106	Eu	LS	10.95	10.65	10.44	10.02	9.80	9.36	-	0.18
107	Eu	LS	-	10.72	10.34	10.07	9.68	9.21	-	0.098
108	Eu	LS	11.0	12.1[b]	11.44	11.04	10.73	10.40	10.06	0.062
				(sixth water wash 9.63)						
109	La	LS	10.95	10.25	9.80	9.22	(very badly peptized)			-
111	Ho	LS	11.1	10.80	10.50	10.16	9.70	9.25	-	0.088
112	Gd	LS	11.0	10.72	10.42	10.06	9.60	9.10	-	0.115
113	Ce	LS	10.95	10.62	10.15	9.40	(badly peptized)			-
115	Eu	LS	10.90	10.60	10.30	10.10	9.62	9.43	8.92	-
118	Eu	LS	10.95	10.78	10.43	10.15	9.72	9.35	9.08	0.109
119	Eu	LS	10.90	10.60	10.35	9.93	9.67	9.28	8.88	0.120

[a] HS = high speed (6000 rpm); LS = low speed (1100 rpm).
[b] First wash with 200 ml of concentrated NH_4OH per gram of metal.

Table 2. Summary of Information on Sols Prepared by the Second Method with a High-Speed Centrifuge in a Glove Box

Sol No.	Metal	Amount of Metal (g)	No. of Centrifuge Tubes	Details of Washes[a]	Final Sol		
					Metal (M)	NO_3^-/Metal Mole Ratio	pH
90	Pr	3	2	10 × H_2O	-	0.21	-
91	Eu	2	2	1 × NH_4OH 6 × H_2O	-	0.14	-
92	Eu	2	2	TMAH ppt., 6 × H_2O	-	0.07	-
93[b]	Pr	3	4	5 × H_2O	0.59	0.20	-
95[c,d]	Pr	1	4	5 × H_2O	0.57	0.19	7.1
96[c,d]	Eu	1	4	4 × H_2O	-	-	-
97[+]	Pr	1	4	5 × H_2O at 0°C	-	-	-
98	Nd	1	4	4 × H_2O	0.485	0.17	-
99	Eu	2	8	4 × H_2O (40-fold excess of NH_4OH)	0.57	0.06	-
100	Eu	2	4	6 × H_2O (40-fold excess of NH_4OH)	-	0.075	-
101	Eu	2	4	7 × H_2O (40-fold excess of NH_4OH)	-	0.080	-
102	Pr	2	4	5 × H_2O (40-fold excess of NH_4OH)	0.66	0.25	7.25
103	Pr	2	4	5 × H_2O	0.725	0.21	-

[a] Twenty-fold excess of NH_4OH used for precipitation except where stated.
[b] NH_4^+ analysis indicated an NH_4^+/Pr ratio of 0.006.
[c] Series of electron micrographs obtained.
[d] For pH of wash liquors, see Table 1.

Table 3. Summary of Information on Sols Prepared by the Second Method with a Low-Speed Preparative Centrifuge in the Laboratory

Sol No.	Metal	Scale (g of metal)	No. of Centrifuge Tubes	Details of Washes[a]	Percentage Loss by Peptization	Final Sol		
						Metal (M)	NO_3^-/Metal Mole Ratio	pH[d]
104	Nd[b]	14.5	4	6 × H_2O (14-fold excess of NH_4OH)	2.6	0.435	0.29	7.4
105	Pr	10	4	5 × H_2O	7.2	0.426	0.24	7.1
106	Eu	10	4	5 × H_2O	6.5	0.41	0.18	9.8
107	Eu	7	4	5 × H_2O	5.7	0.33	0.098	9.5
108	Eu	10	4	7 × H_2O	8.8	0.47	0.062	10.2
110	La	2	1	2 × H_2O[c]	-	-	-	9.6
111	Ho	2	1	5 × H_2O	3.5	0.53	0.088	10.1
112	Gd	2	1	5 × H_2O	6.0	0.53	0.115	10.0
113	Ce	2	1	3 × H_2O[c]	-	-	-	-
115	Eu	8	4	6 × H_2O	8.5	-	-	9.8
118	Eu	8	4	6 × H_2O	-	0.40	0.109	9.7
119	Eu	10	4	6 × H_2O	-	0.50	0.120	-
120	Er	4	2	6 × H_2O	-	0.41	0.093	10.3
121	Nd	4	2	6 × H_2O	-	0.35	0.24	7.45
122	Nd	8	4	6 × H_2O	-	-	-	7.2
123	Pr	10	4	5 × H_2O	-	-	-	(see Fig. 1)

[a] Twenty-fold excess of NH_4OH used for precipitation except where stated.
[b] Carbonate analysis after concentration of sol in rotary evaporator to 0.61 M gave CO_3^{2-}/Nd mole ratio of 0.004.
[c] Final wash badly peptized.
[d] After aging 2 to 3 hr at 25°C.

Table 4. Summary of Information on Sols[a] Prepared by the Second Method and Concentrated by Evaporation

Sol No.	Metal	Scale (g of metal)	Final pH of sol	pH of Sol[b] after 1 hr	Sol after Concentration		Comments
					Metal (M)	NO_3^-/Metal Mole Ratio	
124	Eu	10	9.85	6.6	1.6	-	After concentration for 1 hr at 60°C, sol had a pH of 6.3
127	Eu	10	9.95	6.5	2.5	0.094	
129[c]	Eu	10	9.95	6.5	2.5	-	Enough formic acid added, after sol was formed, to give a formic acid/metal ratio of 0.1.
130[c]	Eu	10	10.12	6.9 immediately on addition of formic acid	2.2	-	Enough formic acid added, after sol was formed, to give a formic acid/metal ratio of 0.4.
131[c]	Eu	10	10.0	6.2	2.5	-	Enough formic acid added during pptn. to give a formic acid/metal ratio of 0.4.
133	Nd	7.5	10.0	6.6	1.9	0.22	Sol thixotropic after concentration
134	Sm	10	10.0	6.8	2.2	-	Sols used to prepare spheres up to 900 μ in diameter.
135	Sm	10	9.9	7.0	2.2	-	
136	Sm	10	10.2	7.0	2.3	0.19	

[a]Sols were prepared with a low-speed centrifuge in the labratory. Four centrifuge tubes and six water washes were used in each experiment.

[b]Sol was at 80°C.

[c]Formic acid added to test effect on size of colloidal particles (see Sect. 3).

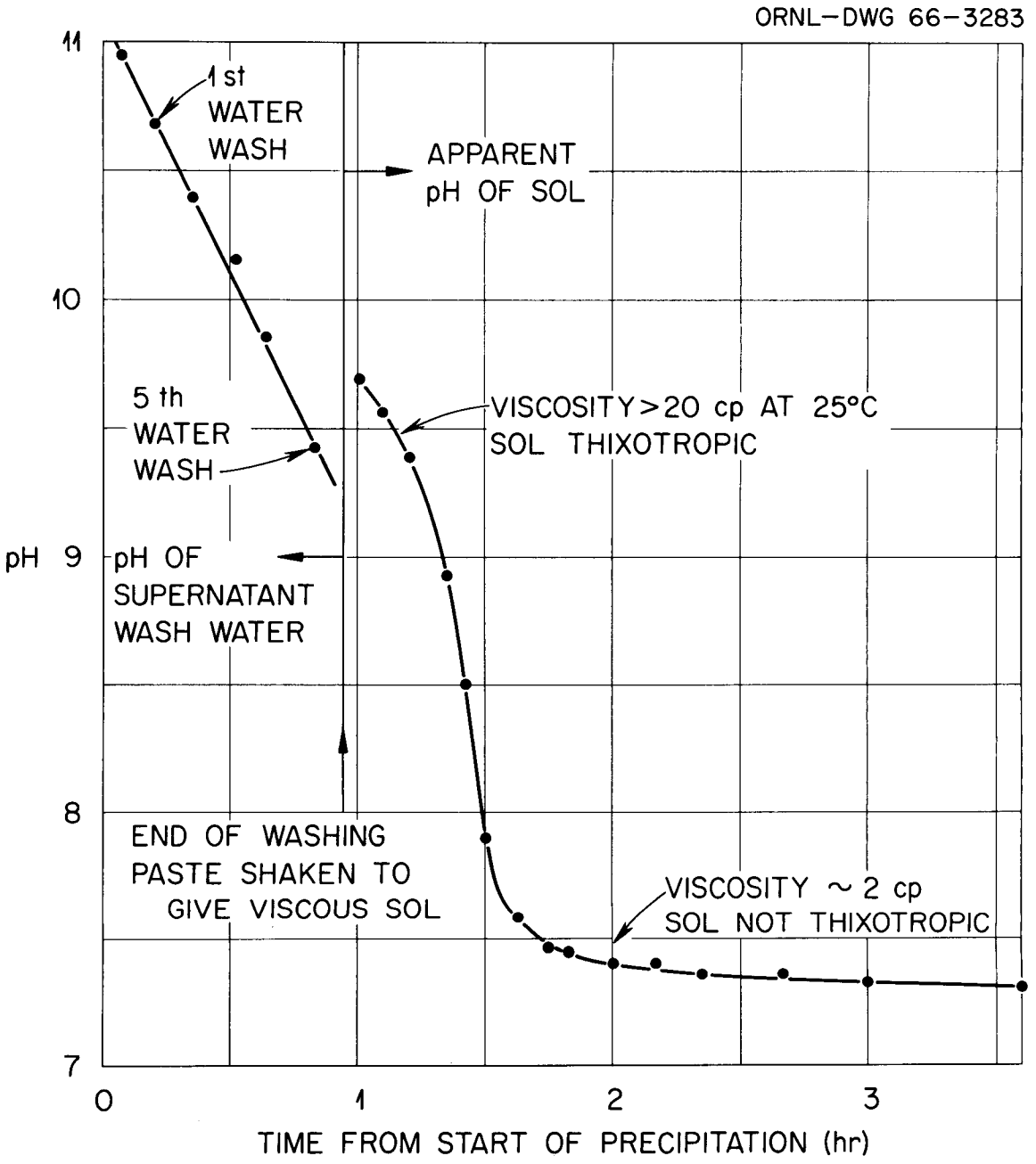

Fig. 1. Variation of pH with Time for Pr Sol 123.

2.2.2. Removal of Nitrate from Lanthanide Hydroxides with Successive Water Washes

The extent of removal of nitrate from a praseodymium hydroxide precipitate was examined (Table 5) as a function of the order of the addition of the reactants in the precipitation stage, the method of aging the precipitate, the number of water washes, and the temperature.

The lowest NO_3^-/Pr mole ratio (0.033) in the final precipitate, coupled with a low loss of Pr by peptization (2.5%), was found in experiment V, batch P (see Table 5), in which the hydroxide was precipitated by adding a 0.2 M praseodymium nitrate solution to a 20-fold excess of 8 M NH_4OH at 25°C. The precipitate was washed once with concentrated NH_4OH and then six times with water. Washing the precipitate with methanol instead of water was less efficient in removing the nitrate (Experiment V, batch Q). Aging the hydroxide in the mother liquor, or in fresh NH_4OH at 0 or 60°C, gave high losses by peptization.

Hydroxide precipitation by the addition of 100% excess TMAH to the nitrate solution at 0°C, followed by four water washes, removed nitrate more efficiently than the addition of the nitrate solution to a 20-fold excess of NH_4OH, followed by four water washes (experiments VI and III, Table 5). However, the product of the TMAH experiment formed poorer gel spheres (milky with rough surface) than did the product from the NH_4OH experiment III (spheres translucent with smooth surface).

X-ray powder patterns were obtained for samples of the damp hydroxide pastes from experiment I, batch A and experiment I, batch D; and crystallite sizes were calculated from the width of the lines (these spectra were poor and showed interference from lines resulting from the Saran plastic film used to protect the samples from CO_2 in the atmosphere).

Sample No.	Aging Time	Crystallite Size (A)
A1	40 min after centrifugation of initial precipitate (no washes)	160 and 300 calculated for two available lines
A7	140 min after precipitation (6 washes with water)	145 and 190 calculated for two lines
D4	1 hr in fresh NH_4OH at 60°C; 2 washes with water at 25°C; total time, 220 min	144 and 180 calculated for two lines

The two, available strong lines in the spectra matched those expected[3] for hexagonal $Pr(OH)_3$, but a broad background signal was also present which decreased in intensity from samples A1 to A7 to D4 and was probably the result of a large proportion of small crystallites (<20 A) or poorly crystalline material.

In experiment III (Table 5), the samples of solid pastes taken for analysis after the third and fourth water washes spontaneously became translucent green sols after about 1 hr. This was our first observation of this behavior with respect to lanthanide hydroxides.

Table 5. Removal of Nitrate from Praseodymium Hydroxide by Successive Water Washes

Expt. No.	Amount of Pr (g)	Temp. of pptn. (°C)	Method of Addition	Batch	Method of Aging	NO_3^-/Pr Mole Ratio						Lanthanide Loss on All Washes (%)
						Initial Supernate	Successive Water Washes					
							1	2	3	4	5	
I	4 (divided into four 1-g batches)	5	50% excess NH_4OH added to Pr	A	None	1.64	0.785 (6th wash, 0.330)	0.529	0.493	0.460	0.462	4.8
				B	5 hr in mother liquor at 0°C	1.23	0.673	0.498	0.475			16.6
				C	3 hr in fresh NH_4OH at 0°C		0.745 (6th wash, 0.414) (7th wash, 0.378)	0.528	0.439	0.421	0.415	17.6
				D	1 hr in fresh NH_4OH at 60°C		0.740	0.334	0.11	0.05		66.7
II	1	60	NH_4OH added to Pr		None	1.10	0.591	0.515	(0.505 with HNO_3 wash, pH 4)			26.1
III	1	25	Pr added to 20-fold excess of 8 *M* NH_4OH		None	0.67	0.366	0.226	0.191	0.173		
V	2 (divided into two 1-g batches)	25	Same as III	P	None	0.65	0.233 (6th wash, 0.033) First wash with NH_4OH	0.092	0.063	0.058	0.055	2.5
				Q	None	0.65	0.233 First wash with NH_4OH; next 4 washes with methanol	0.189	0.173	0.226	0.18	0.65
VI	1	0	100% excess TMAH added to Pr		None	0.66	0.161 All water washes at 0°C	0.114	0.087	0.084	0.090	

2.2.3. Alternative Methods for Washing the Precipitate

The use of a standard centrifuge for separating the precipitate from the wash solutions involved considerable handling of the centrifuge tubes, which is undesirable if the method is to be extended to the preparation of sols of highly radioactive materials. Therefore, we examined (Table 6) two alternative methods: (1) using a basket-type continuous centrifuge with both solid and perforated stainless steel bowls, and (2) filtering the solution through a sintered glass filter.

The conclusions from these exploratory experiments were:

(1) A perforated bowl could not be used satisfactorily in the continuous centrifuge, using filter-paper strips as the filter, because the water did not wash the precipitate efficiently (i.e., to a low residual NO_3^-/metal mole ratio of less than 0.2) except in the vicinity of the holes. Only about half of the precipitate formed a fluid sol spontaneously, whereas, with the usual method of centrifugation, 100% of the precipitate formed a fluid sol.

(2) To obtain efficient washing of the precipitate in the solid bowl, it was necessary to slurry the precipitate with water each time, remove it from the bowl, and add it again when the bowl had attained speed. In experiments with Eu, extensive peptization was observed in the washes after the fourth wash. The washed precipitate was easily converted into fluid sol by heating the bowl for 1 hr at 80°C in a water bath. The Eu concentration in resulting sols was increased from 0.4 to 2.5 M by placing the sol in a rotary vacuum evaporator for about 45 min at 60°C. The NO_3^-/metal mole ratio (0.108, sol 128; 0.24, sol 116) was of the same order as that obtained by the standard method.

(3) Filtration through a sintered-glass filter was the simplest method and required a relatively small amount of water to reduce the pH of the filtrate to less than 9. However, the method was slow because of the partial blockage of the filter with fine particles; in future work, it may be necessary to use a filter aid such as Celite (Johns Manville Co.) to increase the rate of filtration. The precipitate was readily converted into a fluid sol *in situ* by heating the filter for 1 hr at 80°C.

2.2.4. Charge on the Sol Particles

Measurements in a Tiselius electrophoresis apparatus showed the particles of a Pr sol (No. 105) to be positively charged. The apparent pH of the sol (0.43 M in Pr), as well as the pH of the dialyzed interparticle fluid, was $\overline{7}.2$.

This result lends support to the early assumption that these lanthanide hydroxide sols were positively charged colloids, probably with nitrate counterions. It is possible that both nitrate and hydroxide ions contribute to the electrical double-layer around the positively charged hydroxide particle.

Table 6. Summary of Information on Sols Prepared by Using a Continuous Centrifuge and by Filtration

Sol No.	Metal	Amount of Metal (g)	Method	pH of Wash Liquor After Successive Washes							Total Volume of Wash Water (liters)	Comments
				1	2	3	4	5	6	7		
116	Pr	10	Perforated bowl; centrifuge at 4000 rpm	10.6	10.5	10.4	10.3	10.2	9.2	8.9	3.5 in seven 0.5-g batches	NO_3^-/Pr ratio = 0.24; only part of ppt. changed to sol (0.43 *M*) spontaneously
117	Pr	10	Perforated bowl; centrifuge at 4000 rpm	10.1	9.7	9.2	8.1	8.1			5 in five 1-g batches	
125	Pr	10	Solid bowl; centrifuge at 4000 rpm	10.6	10.4	10.1	9.6	9.2			4 in five 0.8-g batches	Final pH of sol was 7.6
126	Eu	10	Solid bowl; centrifuge at 4000 rpm	10.8	10.5	10.4	10.1	9.8	9.4	8.9	5.6 in seven 0.8-g batches	Ppt. scraped out and heated 1 hr at 80°C
128	Eu	10	Solid bowl; centrifuge at 4000 rpm	10.7	10.5	10.4	10.1	9.8	9.3		4.8 in six 0.8-g batches	Heated bowl 1 hr at 80°C. Sol concentrated to 2.5 *M* in rotary evaporator, pH 6.3
132	Eu	5	Medium glass filter with lab. vacuum	Final pH = 8.6							2	Filter heated 1 hr at 80°C to liquefy sol

2.3. Miscellaneous Methods

2.3.1. Thermal Denitration of Praseodymium Nitrate Hydrate

Praseodymium nitrate hydrate (5 g) was heated slowly in a porcelain dish over a Meker burner. The solid melted in its water of crystallization, solidified, remelted at about 300°C, evolved brown fumes, and then resolidified. The resulting chocolate-brown solid, which was subsequently ground to a powder, gave an infrared spectrum that indicated the presence of a substantial amount of nitrate. The powder was heated for 30 min at about 500°C, during which time it evolved brown fumes and became darker in color. Its weight at this stage corresponded closely to that expected for Pr_6O_{11}, but a small amount of nitrate still remained. The solid was suspended in CO_2-free water containing 0.06 mole of nitric acid per mole of Pr and was heated with stirring for several hours, but it could not be peptized to form a sol.

Another sample of 5 g of praseodymium nitrate was heated in a muffle furnace for 2 hr at 300°C, and then for an additional 1.5 hr at 500°C. The resulting chocolate-brown oxide was suspended in water containing 0.04 mole of nitric acid per mole of Pr and heated, with stirring, at 60°C for several hours; however, it could not be peptized to form a sol. Denitration in steam may give more satisfactory products than were obtained by the methods described above.

2.3.2. Amine Extraction of Nitrate from a Solution of Praseodymium Nitrate

Extraction of nitrate from a 0.1 M solution of praseodymium nitrate in water with a solution of 20 vol % Primene JMT in benzene gave a hydroxide precipitate that was difficult to centrifuge down because of the formation of a foam. The precipitate was washed, first, with benzene (to remove amine), and, secondly, with water; it was then stirred in water at about 60°C for 1 hr to produce a sol that was about 1 M in Pr. Microspheres were formed by injecting this sol into a stirred mixture of 80 vol % 2-ethylhexanol–20 vol % 2-octanol. After 15 min, the spheres were filtered off, washed with methanol, and dried at 100°C for 15 min; a large proportion of them were broken and had a foamlike internal structure. The intact spheres were whitish-green and had a low resistance to crushing; the NO_3^-/Pr mole ratio was 0.32. The spheres contained some organic matter (e.g., benzene or amine), which probably prevented the formation of good spheres. This method of sol preparation does not appear to be promising because of the difficulty of removing entrained amine from the product.

2.3.3. Methods of Preparing Hydroxide Sols by Slow Precipitation

The slow, homogeneous precipitation of praseodymium hydroxide with ammonia that is liberated from the decomposition of urea in solution at the boiling point was examined. A solution of 10 millimoles of praseodymium nitrate in 55 ml of water was boiled under reflux for 9 hr with 1.08 g of urea (20% excess over the stoichiometric amount). A pale, greenish-white precipitate formed at a constant pH of 4.5, and this was centrifuged down and washed twice with distilled water. The resulting solid was suspended in 20 ml of water and heated for 35 min, but it readily sedimented

and showed no signs of peptizing; a sample was removed and dried at 120°C for 1 hr. An infrared spectrum of the dried solid in a KBr disk showed it to consist substantially of praseodymium carbonate (with no trace of nitrate present). Apparently, carbon dioxide had been absorbed from the decomposition of the urea.

To obtain slow precipitation without the absorption of carbon dioxide, another method was tested. Praseodymium hydroxide was precipitated slowly (over a period of 1.5 hr) by bubbling nitrogen first through a solution of 10 M ammonium hydroxide and then through the solution of praseodymium nitrate (15 millimoles in 150 ml). The pH of the latter solution remained at 7.5 until about 90% of the praseodymium had been precipitated, and then increased to 9.5. The precipitate was centrifuged and washed five times with water; the last wash was left in contact with the solid overnight. The pH of the wash solutions decreased as follows: 9.3, 9.1, 8.7, 7.5, 6.0 (heavily peptized). The solid was resuspended in 20 ml of water and mixed, using a vibratory mixer, for 10 min. The pH of the suspension was 7.5; 0.5 millimole of nitric acid was added, and the suspension was heated at 60 to 70°C for 1 hr. Before nitric acid was added, a small volume of the suspension was removed and dried at 130°C for 30 min. The infrared spectrum of this solid was similar to the spectra obtained previously on solids precipitated rapidly with ammonium hydroxide. A 1-ml sample of the suspension was analyzed spectrophotometrically for nitrate and was found to have an NO_3^-/Pr mole ratio of 0.33. Microspheres were formed by the beaker method when the sol had a creamy consistency (Pr concentration, ~0.8 M), washed with methanol, and dried for 2.5 hr at 120°C. The spheres had an irregular shape and rough surface, and the interior had a "plastic foam" appearance, similar to that found previously with other sols having a high NO_3^-/Pr ratio. Nitrate is, therefore, removed less efficiently from precipitates formed by this very slow method of precipitation than from precipitates formed by rapid precipitation with a solution of either NH_4OH or TMAH.

2.4. Spectra of Sols and Solutions Derived from Sols

2.4.1. Determination of the Concentrations of Lanthanide Metal and Nitrate

The concentrations of metal ion and nitrate in sols, gels, and microspheres of lanthanide hydroxide were measured simply and rapidly by dissolving 50 to 100 mg of solid sample, or 1 to 2 ml of sol, in 3 to 5 ml of dilute perchloric acid, adjusting the perchloric acid concentration to about 1 M, and measuring the spectra in a 1-cm cell vs water in the region 2800 to 6500 A.

The wavelengths and molar absorptivities of the various bands (measured for solutions prepared by dissolving weighed amounts of freshly calcined oxides in perchloric acid) are given in Table 7.

The following formula, which was used to correct the observed optical density (O.D.) for nitrate at 3000 A for the contribution of the Eu^{3+} uv band, was developed from the spectrum of a solution of Eu^{3+} in 1 M perchloric acid:

Corrected O.D. (NO_3^-) = observed O.D. (at 3000 A) − 0.157·O.D. (at 3935 A), in which the observed O.D.'s are corrected for background absorption.

Table 7. Wavelengths and Molar Absorptivities of the Bands Characteristic of Lanthanide Ions and Nitrate in Perchloric Acid

Ion	Band Maximum (A)	Molar Absorptivity	Band Shape	Interference with Nitrate
Pr^{3+}	4440	10.1	Singlet, sharp	None
Nd^{3+}	5740	7.2	Multiplet, sharp	Two very weak peaks superimposed on NO_3^-
Gd^{3+}	2740	0.6	Singlet, sharp	Superimposed on NO_3^-; very poor sensitivity
Eu^{3+}	3935	2.42	Singlet, sharp	Needs correction (see text below)
Ho^{3+}	5360	3.44	Singlet, sharp	Slight interference by peaks <3000 A
Sm^{3+}	4015	3.30	Singlet, sharp	None
NO_3^-	3000	7.3	Singlet, broad	---

The presence of droplets of an organic drying solvent or of an amine used for denitration gave a cloudy solution; thus these impurities had to be removed by washing the solution twice with an equal volume of benzene and then blowing air through the solution for 15 min to remove the traces of benzene.

2.4.2. Reflectance Spectra of Microspheres of Neodymium-Praseodymium Oxides

The measurement of reflectance spectra in the visible region was evaluated as a potential direct method for the determination of the NO_3^-/metal mole ratio and of the relative amounts of metals in microspheres. Microspheres containing Nd^{3+}, Pr^{3+}, and NO_3^- were selected because of the numerous intense, sharp absorption peaks of these metal ions in the 3000- to 10,000-A region. Samples of about 100 mg of 100- to 200-μ-diam microspheres of mixed Nd-Pr oxides-hydroxides both before and after firing at 1100°C were examined in a Cary model 14 spectrophotometer that was fitted with a reflectance attachment. The absorption spectrum of a sample of the unfired microspheres dissolved in 1 M perchloric acid was measured in the same region, using a 1-cm silica cell in a similar Cary model 14 spectrophotometer. The fired microspheres, which were black, gave only a continuous reflection spectrum over the available range of 2500 to 7500 A; this will not be discussed further.

Based on the absorption spectrum of the solution and published extinction coefficients of the peaks at 5220 and 5756 A (Nd) and at 4442 and 4818 A (Pr), the Nd^{3+}/Pr^{3+} mole ratio was 1.77, which is equivalent to 64 mole % Nd, and the NO_3^-/(Nd + Pr) mole ratio was 0.020. All the peaks

in the reflection spectrum were shifted to the red with respect to the absorption spectrum of the solution, the mean shifts being 56 ± 7 A for Pr and 36 ± 12 A for Nd. Multiple bands were resolved to a higher degree in the reflection spectrum; for example, five peaks plus a shoulder were observed in the region 5000 to 5400 A for the absorption spectrum of the solution, corresponding to eight peaks plus a shoulder in the reflection spectrum. Shifts of this order, and splitting of bands, have been reported previously[4] for Pr complexes [e.g., $Pr(OH)_3$], compared with the aquo-ion.

The relative intensity of each peak, expressed as optical density for the reflection peak divided by the optical density for the absorption peak (1-cm cell), varied from 0.7 for the Nd^{3+} peak at 7454 A to 3.0 for the Pr^{3+} peak at 5943 A, and no correlation with wavelength or element was apparent. This unexpectedly large variation of relative intensity at different wavelengths made the measurement of reflectance spectra unsuitable for the direct analysis of the NO_3^-/metal mole ratios, or of the mole ratios of different metals, without more extensive measurements and careful calibration. The variation was probably the result of the different degrees of resolution of the multiple bands in absorption and reflection.

2.4.3. Ultraviolet and Visible Spectra of Sols of Praseodymium Hydroxide, and Measurement of Particle Size

Sols 0.005 to 0.5 M in praseodymium hydroxide, and having an NO_3^-/Pr mole ratio of 0.06 to 0.25, gave sharp absorption bands at 4487, 4740, 4872, 5934, and 6042 A superimposed on a smooth curve (Fig. 2). The absorbance was inversely proportional to approximately the fourth power of the wavelength. The absorption peaks were intensified by a factor of 1.4 to 2.3, and the wavelengths of the peaks were shifted by an average of +62 A relative to the values for the aquo-ion in 1 M perchloric acid. The $^1D_2$ transition of the ion at 5890 A was split into two distinct peaks. These red shifts agreed closely with those found in the reflection spectra of the solid gel microspheres (Sect. 2.4.2.).

The molecular shape and size of sol particles can be calculated from measurements of the scattering of light by a sol.[5] The two principal methods are based on the measurement of (1) light scattered at 90° (or some other angle) to the incident beam, using a light-scattering photometer, and (2) the decrease in the intensity transmitted along the axis of the beam, in a conventional spectrophotometer. The latter method is more simple, experimentally, and has been evaluated for the rare-earth hydroxide sols, as well as for thoria sols and plutonium polymer.

The conditions that must be satisfied for the application of simple mathematical expressions to the calculation of molecular weight are: (1) the sol particles should have a diameter less than $\lambda/20$, where λ is the wavelength of the incident light; (2) the particles should be isotropic; (3) the decrease in light intensity should be the result of scattering and not of absorption; (4) the turbidity (τ), which is proportional to the optical density, should be related linearly to the concentration of the sol particles; (5) the term $\tau\lambda^4$ should be constant with λ (variation of this term may indicate absorption); and (6) a log-log plot of τ vs λ should be linear with a slope of −4 (slopes of less than −4 require a more complicated mathematical treatment).

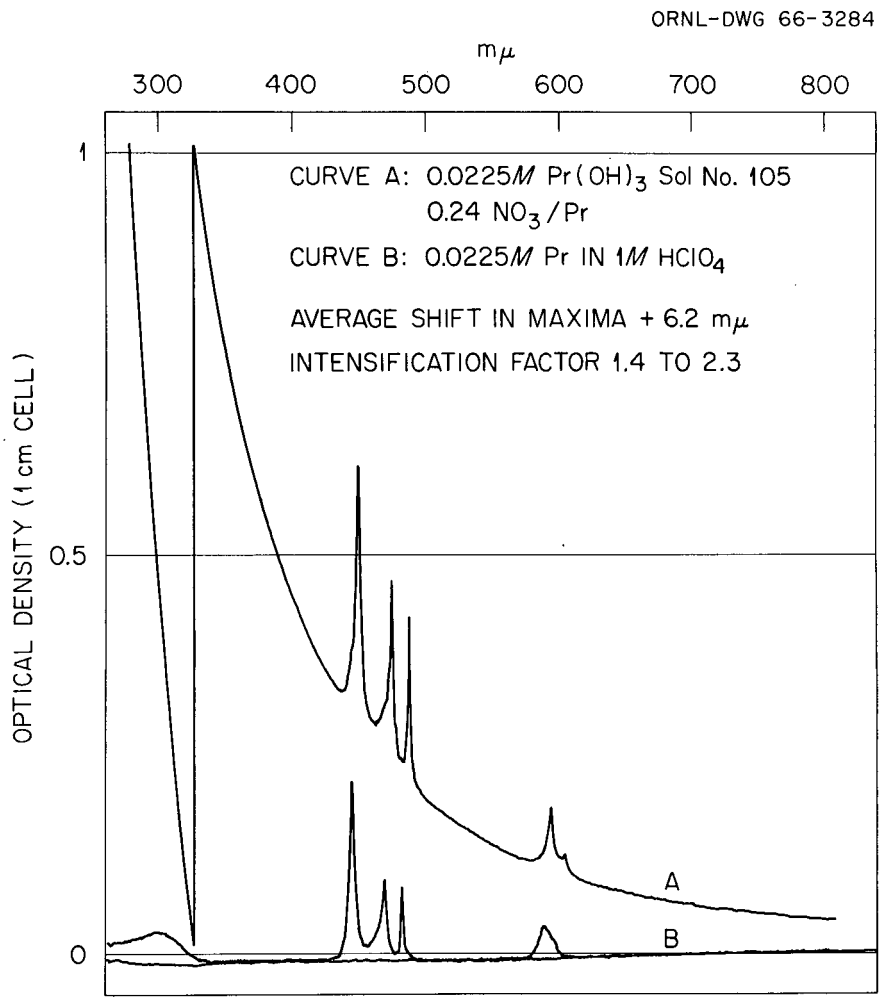

Fig. 2. Spectra of Praseodymium Hydroxide Sol and Praseodymium Perchlorate Solution.

The following basic equations[5,6] were used to calculate the weight-average molecular weight (M) and radius (r) of a sol particle:

$$M = \frac{3\tau N\lambda^4 c}{32\pi^3 n_0{}^2 (n - n_0)^2} = \frac{1.026 \times 10^{21} \tau \lambda^4 c}{(n - n_0)^2} ,$$

where

τ = 2.303 times the optical density in a 1-cm cell,
λ = wavelength in cm,
c = concentration of the sol in g/cc,
N = Avogadro's number,
n_0 and n = refractive indexes of the solvent and the sol at wavelength λ;

and

$$r^6 = \frac{3\tau\lambda^{*4}M(m^2 + 2)^2}{128\pi^5\ Nc(m^2 - 1)^2},$$

where

$$\lambda^* = \lambda/n_0,$$
$$m = n_{solute}/n_{sol}.$$

The variation of τ (corrected for absorption) with λ and c for sols 0.09, 0.02, and 0.005 M in Pr showed that: (1) τ was linearly related to c only up to about a concentration of 0.02 M, above which it decreased with c (13% low at 0.09 M); (2) $\tau\lambda^4$ was constant $(2.21 \pm 0.14) \times 10^{-12}$ from 6500 to 2500 A for the 0.02 M sol; (3) the exponent of the plot of log τ vs log λ was -3.83 ± 0.18. Hence, the conditions for the calculation of M and r from the results were satisfied approximately, provided that an extrapolation to zero concentration was used to correct for the nonlinear variation of τ with c. The calculation of r required either the measurement of the refractive index of the sol particles or the assumption of some model of the dimensions and molecular weight of the "monomer."

A value of the refractive index increment (change in refractive index per unit change in concentration) of 0.034 $mole^{-1}$ liter was obtained with a Zeiss dipping refractometer using white light. This value, together with a value of 1.75 for the refractive index (n_{solute}) of the sol particles, which was obtained by analogy with other rare-earth hydroxides,[2,7] was used in the calculation of molecular weights and radii of particles for the sols referred to in Sect. 2.1.3.

No estimate of the shape of the particles could be obtained from the simple turbidity measurements; however, more lengthy experiments with a light-scattering photometer would enable the shape to be determined. The electron micrographs (Sect. 3) showed that the assumption that scattering particles were spherically symmetrical was not justified (unless large aggregates of randomly oriented needle-shaped crystals were present); likewise, the assumption that all particles were about the same size (the effect of a small proportion of large diameter scattering particles is very great) was found to be incorrect. It seems likely, therefore, that the calculated molecular weights and particle diameters are probably only correct to an order of magnitude with this particular system, and that direct electron microscopy offers more promise for future work than does a light-scattering method.

2.4.4. Infrared Spectra of Various Sol-Gel Materials

We used a Perkin-Elmer Infracord spectrometer to measure the infrared spectra, in the range 2.5 to 15 μ, of two types of samples: (1) solids that had been pressed into pellets with potassium bromide and ground up as

mulls with Nujol, and (2) sols and gels that were held as thin films between silver chloride plates. Organic matter (e.g., residual tetramethylammonium ions, or long-chain alcohols used to dry the sols) was detected in some batches of microspheres by the C-H stretching vibrations in the 3- and 7-μ regions. The absorption of CO_2 by a sol or gel was also detected by the C-O stretching vibrations at 6.7, 7.1, and 11.3 μ, except that there was interference in the 7-μ region when a large amount of nitrate was present.

The residual nitrate showed up clearly in the gel microspheres as strong bands at 6.7 and 7.3 μ and as a weaker band at 9.4 μ (the 7.3-μ band in KBr disks arises from nitrate ions produced by reaction of the sample with the KBr to give KNO_3). The bands were similar to those found in solid praseodymium nitrate hydrate and arise from nitrate groups coordinated to the metal, not from nitrate ions. In sols, the nitrate bands were broader and subject to interference from the strong band of water at 6.1 μ. Calcined oxides had a featureless spectrum from 2.5 to 15 μ; observation at higher wavelengths may be useful in that it may reveal the metal-oxygen stretching bands.

Disadvantages of the Infracord spectrometer are that (1) it heats up the sample in the beam to 50 to 70°C, depending on the absorptivity of the sample, and (2) it is not sufficiently sensitive to detect traces of impurities (e.g., carbonate or organic matter) that may affect the properties of the sols.

Infrared spectra of hydrated nitrates and carbonates of Pr, Nd, and Eu were measured as a function of the temperature to which the samples were heated (see Sect. 5).

3. ELECTRON MICROSCOPY AND ELECTRON DIFFRACTION OF SOLS

Samples of hydroxide sols of Pr, Nd, and Eu were examined by electron microscopy to determine the shape and size of the colloidal particles at various stages in the second method of preparation (Sect. 2.2). Electron diffraction measurements were made on selected 1 μ × 1 μ areas of the sols to ascertain the amorphous or crystalline form of the particles.

3.1. Preparation of Samples and General Results

Each sample, containing a fraction of a milliliter of sol, was diluted about 100-fold with CO_2-free distilled water. One drop of this dilute sol was placed on a Formvar-covered copper grid and inserted in the electron microscope (Phillips type EM2). The image was observed on the screen about 10 min after sampling, and negatives were prepared on plates. The details of the samples that were examined are given in Tables 8 and 9; the shapes and sizes of the particles were measured from 10 × 8 in. photographic prints at a final magnification of 165,000 ×.

Table 8. Sols[a] Examined by Electron Microscopy

Metal	Sol Sample No.	Fig. No.	Preparation and Treatment Procedure	Time of Aging at 25°C from Precipitation to Electron Microscopy	Size, Shape, and Crystallinity of Particles
Pr	95-1	3A	Freshly precipitated hydroxide centrifuged from mother liquor; 20 times excess NH_4OH used for ppn.	18 min	30-60 A; spherical, amorphous; a few isolated rods 480 to 580 A long and about 60 A wide
Pr	95-2	3B	Ppt. washed 5 times with H_2O, with intermediate stirring and centrifuging; NO_3^-/Pr = 0.19	80 min	Amorphous particles and in sol 95-1; also crystalline rods 300 to 700 A long and 30 to 90 A wide
Pr	95-3	3C	Similar to that for 95-2; aged additional 60 min until liquefied to translucent sol; Pr = 0.57 *M*	140 min	All crystalline rods, single or as bundles, 400 to 1000 A long and 20 to 200 A wide
Pr	90	3D	Prepn. similar to that for sol 95; except 40 times excess NH_4OH used for pptn. and ppt. washed ten times with H_2O; NO_3^-/Pr = 0.21	6 days	All rods or bundles, as in sol 95-3; same size ranges
Eu	96-1	4A	Freshly precipitated hydroxide centrifuged from mother liquor	20 min	30 to 60 A; spherical, amorphous
Eu	96-2	4B	Ppt. washed 4 times with H_2O; solid paste	80 min	30 to 200 A; spherical; probably agglomerates of smaller particles
Eu	96-4	4D	Same as that for 96-2; kept over weekend	67 hr	Many small amorphous particles; many bundles of crystalline rods from 1500 to 7500 A long and 100 to 600 A wide
Eu	99-1	4C	Similar to that for sol 96, but aged 25 hr at 25°C. Very thixotropic, translucent liquid sol; NO_3^-/Eu = 0.06	25 hr	Amorphous particles; bundles of rods 700 to 4000 A long and 60 to 300 A wide

[a]Sols are shown in Figs. 3 and 4.

Table 9. Sols[a] Examined by Electron Microscopy

Metal	Sol Sample	Preparation and Treatment Procedure	Aging Conditions		Size, Shape and Crystallinity of Particles
			Time (hr)	Temperature (°C)	
Pr	93	Similar to that for sols 90 and 95, but 40 times excess ammonia used for pptn.; NO_3^-/Pr = 0.20 after 5 washes with H_2O	4	Heated, 60	All crystalline rods[b] 300 to 1200 A long and 30 to 200 A wide
Pr	97-1	Similar to that for sol 95, but pptn. and all washes at 0°C; solid paste	2	0	Some amorphous particles[c]; some crystalline rods[c] 400 to 700 A long and 30 to 90 A wide
Pr	97-2	Similar to that for sol 97-1, but HNO_3 added to give an HNO_3/Pr ratio of 0.1 after 2 hr at 0°C; liquefied sol aged additional 3 hr at 0°C	5	0	All crystalline rods,[b] single or as bundles, 400 to 2000 A long and 20 to 200 A wide
Pr	97-3	Similar to that for sol 97-1, but liquefied	6	0	All crystalline rods[b] 400 to 1000 A long and 20 to 200 A wide
Eu	99-2	Compare with sol 99-1 (Table 8); HNO_3 added to give an NO_3^-/Eu ratio of 0.16; milky-white color	25	25	Less amorphous material than that from sol 99-1, but larger bundles of crystalline rods up to 4500 A long and 700 A wide
Nd	104	Standard method, 14-g scale (see Table 3); ultrasonically dispersed	24	25	Crystalline rods from 300 to 1800 A long and 20 to 160 A wide

[a]Sols are not illustrated.
[b]Similar to those in sol 95-3 (see Table 8).
[c]Similar to those in sol 95-2 (see Table 8).

Electron micrographs of the praseodymium hydroxide and europium hydroxide sols (Figs. 3 and 4 respectively) show the effect of aging time. Electron diffraction patterns from selected areas of the grid are shown in Figs. 5 and 6.

Electron diffraction data for the crystalline hydroxides of Pr, Nd, and Eu (sols 95, 104, and 96 respectively) obtained from the electron diffraction plates are presented in Table 10. The spacings of the diffraction lines agree very closely with the x-ray data reported for $Nd(OH)_3$,[7] and $Eu(OH)_3$[2] (and differ significantly from those expected for Eu·O·OH). The intensities are different from those reported for the x-ray measurements, but this is not unusual since the rods in our preparations appear to have preferred orientation.

ORNL DWG 67-1577

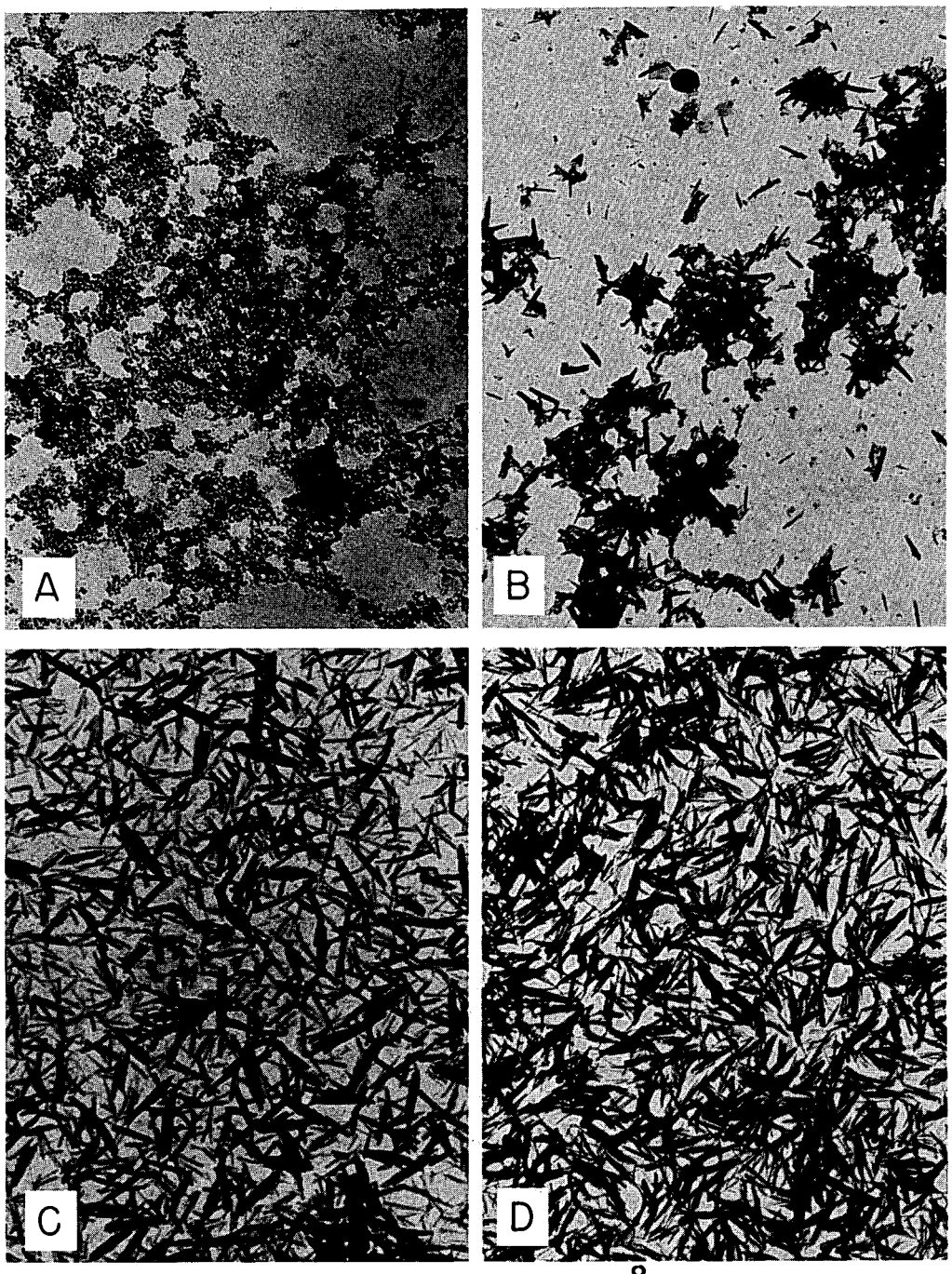

SCALE ⊢ = 600 Å

A - FRESHLY PRECIPITATED, AGED 18 min.

B - PRECIPITATE WASHED, AGED 80 min.

C - PRECIPITATE WASHED, AGED 140 min.

D - PRECIPITATE WASHED, AGED 6 days

Fig. 3. Electron Micrographs of Praseodymium Hydroxide Sols.

ORNL DWG 67-1578

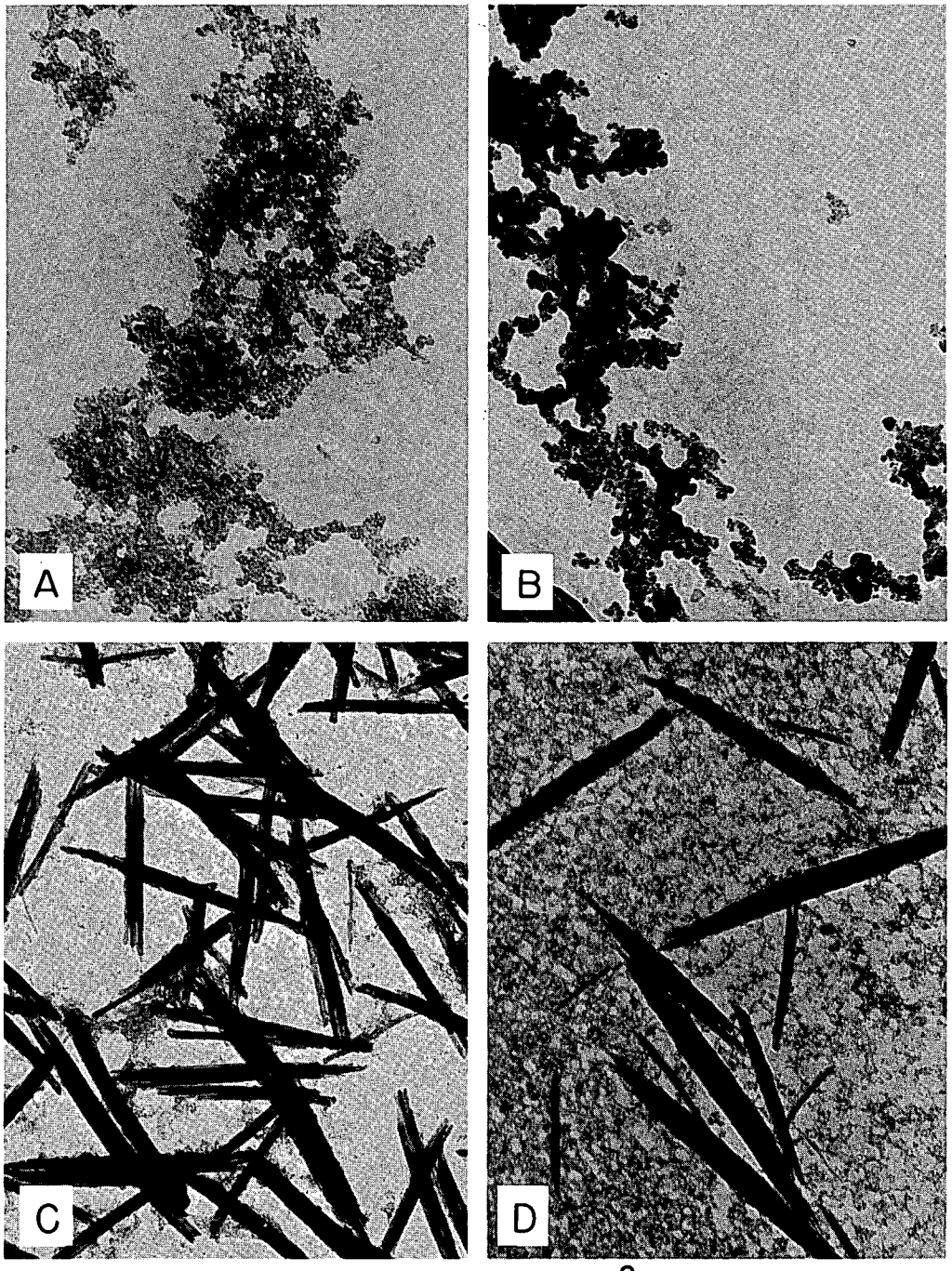

SCALE ⊢ = 600Å

A - FRESHLY PRECIPITATED, AGED 20 min.

B - PRECIPITATE WASHED, AGED 80 min.

C - PRECIPITATE WASHED, AGED 25 hrs.

D - PRECIPITATE WASHED, AGED 67 hrs.

Fig. 4. Electron Micrographs of Europium Hydroxide Sols.

PHOTO 83062

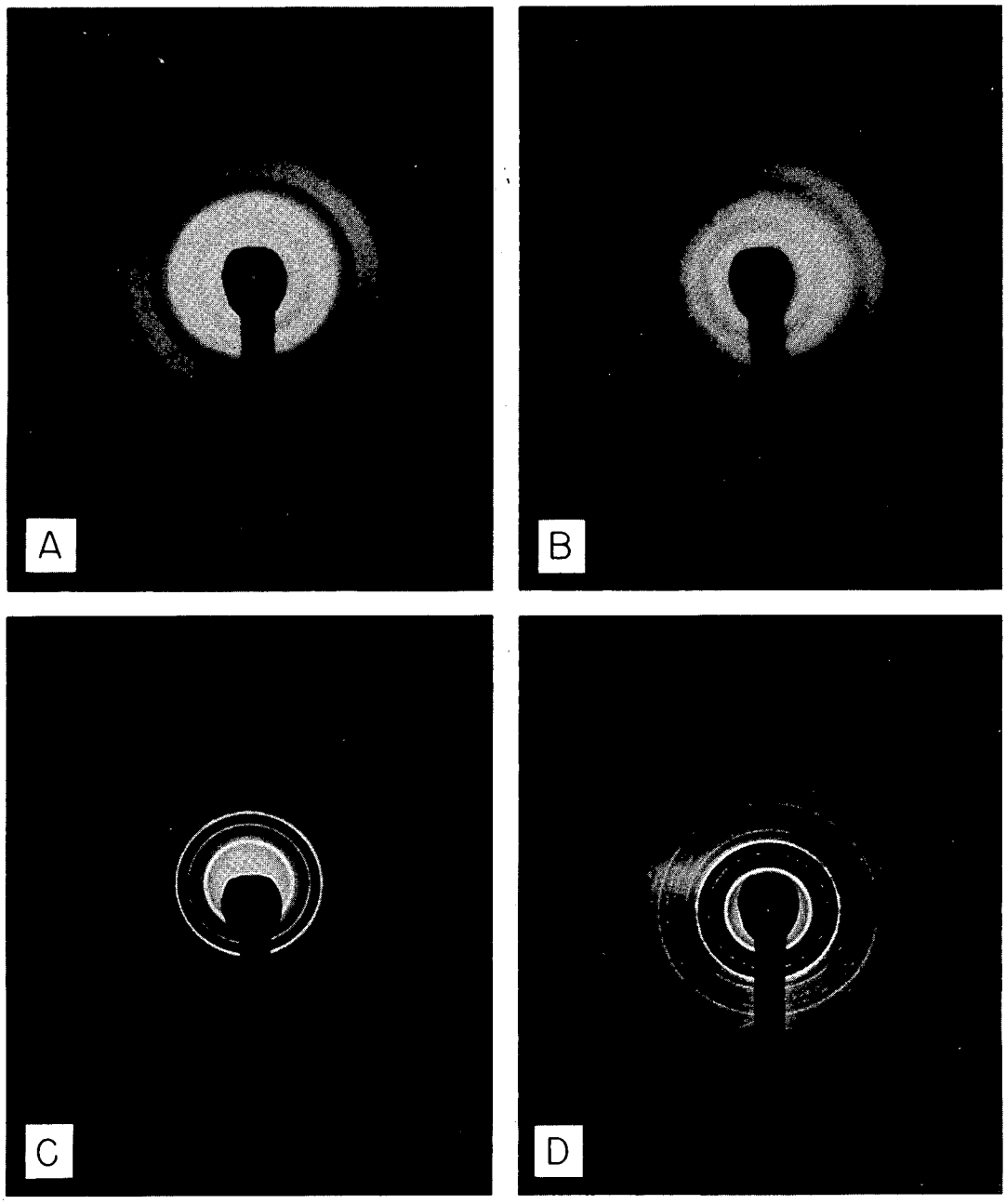

A - FRESHLY PRECIPITATED, AGED 18 min.
B - PRECIPITATE WASHED, AGED 80 min.
C - PRECIPITATE WASHED, AGED 140 min.
D - PRECIPITATE WASHED, AGED 6 days

Fig. 5. Electron Diffraction Patterns of Praseodymium Hydroxide Sols.

PHOTO 83063

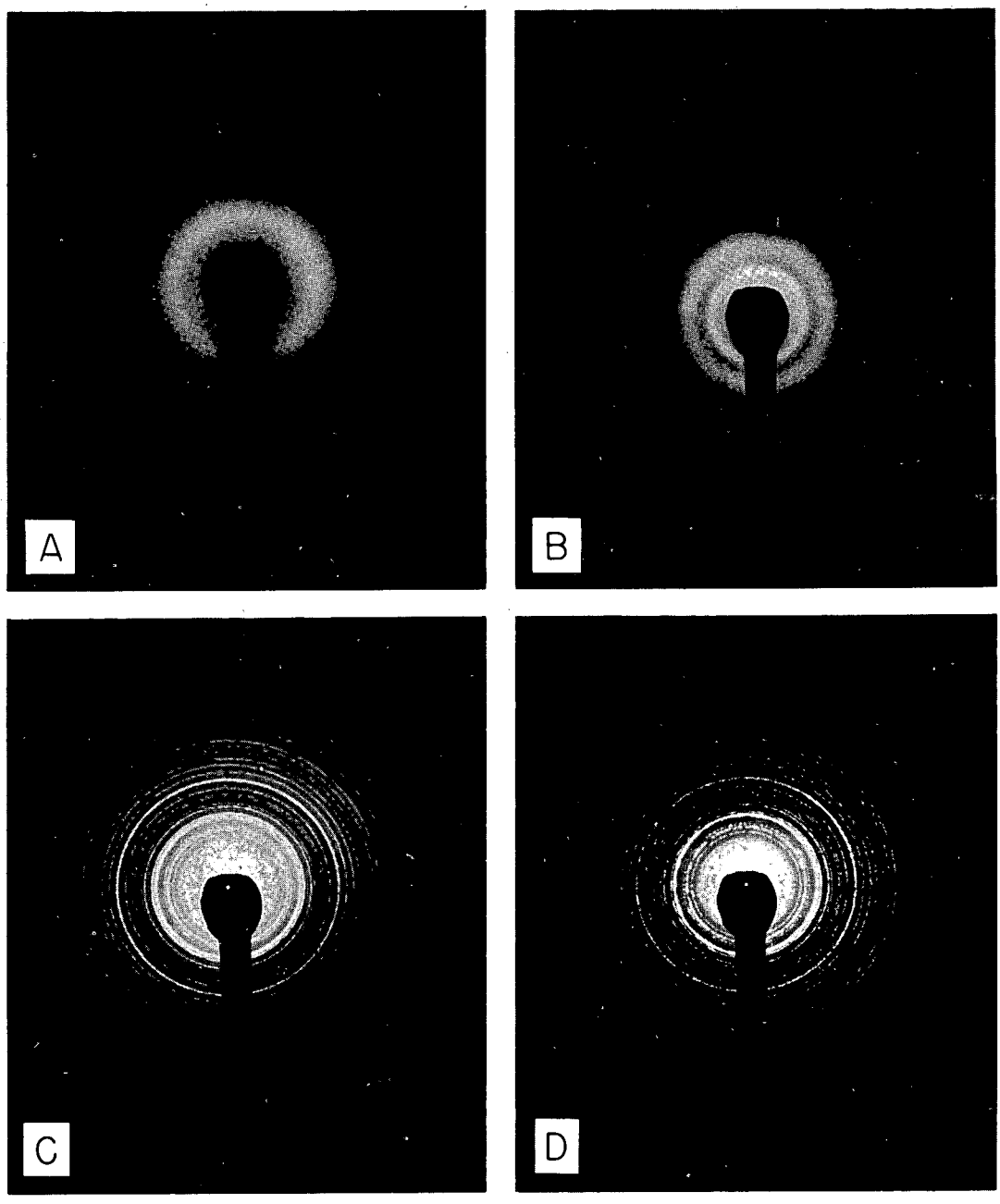

A - FRESHLY PRECIPITATED, AGED 20 min.
B - PRECIPITATE WASHED, AGED 80 min.
C - PRECIPITATE WASHED, AGED 25 hrs.
D - PRECIPITATE WASHED, AGED 67 hrs.

Fig. 6. Electron Diffraction Patterns of Europium Hydroxide Sols.

Table 10. Electron Diffraction Data for Hydroxides of Pr, Nd, and Eu

hkl	$Pr(OH)_3$[a] Data from Diffraction Pattern of Sol 97-3		$Nd(OH)_3$[b] Data from ASTM X-Ray Card 6-0601 (ref. 7)		$Nd(OH)_3$[b] Data from Diffraction Pattern of Sol 104		$Eu(OH)_3$[c] Data from Literature (X-Ray) (ref. 2)		$Eu(OH)_3$[c] Data from Diffraction Pattern of Sol 96-4	
	d (A)	I/I_0 (ref. d)	d (A)	I/I_0	d (A)	I/I_0 (ref. d)	d (A)	I/I_0	d (A)	I/I_0 (ref. d)
100	5.559	M	5.57	80	5.57	M	5.52	70	5.52	M
110	3.193	M+	3.20	65	3.20	M+	3.184	55	3.18	M+
101	3.077	VS	3.08	85	3.08	VS	3.047	100	3.05	S
200	2.765	W+	2.768	10	2.768	W+	2.757	20	2.758	W+
111	2.447	W+	2.45	5	2.45	W+	2.399	5	2.40	W+
201	2.216	S–	2.217	100	2.217	S	2.202	50	2.204	S
210	2.088	VW	2.092	10	2.092	VW	2.083	6	2.08	W+
300	1.844	S	1.848	50	1.848	S	1.837	15	1.84	VS
002	1.832	M+	1.842	100	1.842	M+	1.828	20	1.822	S
211	e				e		1.810	35	e	
102	1.767	M			1.764	M	1.733	6	1.740	M
220	1.601	M	1.605	30	1.605	M	1.589	2	1.588	M–
112	e				e		1.585	14	e	
310	1.536	W	1.540	10	1.54	W	1.527	4	1.52	W
202	e				e		1.524	4	e	
311	1.413	W+	1.417	20	1.417	W+	1.410	8	1.41	W+
212	e		1.392	10	e		1.374	5	1.374	W
302	1.307	W+	1.311	15	1.29	W	1.295	7	1.292	W+
320	e		1.29	10	e		1.262	1	e	
410, 222	1.209	W+			1.201	W+	1.201	10	e	
321	e				e		1.194	10	1.192	W+
103	e				e		1.189	2	e	
312	e				e		1.171	2	1.168	W
203	1.132	W			1.125	W	1.113	4	1.114	W

[a]Parameters for hexagonal structure[3]: a = 6.48 A, c = 3.77 A.
[b]Parameters for hexagonal structure[7]: a = 6.421 A, c = 3.74 A.
[c]Parameters for hexagonal structure[2]: a = 6.421 A, c = 3.645 A.
[d]Visual.
[e]Missing or unresolved lines.

3.2. Detailed Structure of Colloidal Crystals of Lanthanide Hydroxides

The rod-shaped crystals observed on the electron micrographs showed many similarities to those of β-FeO·OH, which were studied in detail recently by Watson and co-workers.[8] The particles appeared to lie flat on the grids, and no information could be obtained concerning the dimensions of the particles in the direction of the beam. Thus other methods were used; in addition, several grids were examined at magnifications up to 658,000 × in an attempt to resolve the structure of the individual rods.

3.2.1. Stereoscopic Electron Micrography

Two negatives of the same field of view [$Eu(OH)_3$ sol] were exposed with the angle of the electron beam shifted by 6°. The final prints were aligned by trial and error to give the maximum stereoscopic effect in a hand viewer. (The field is not identical in each because of small shifts caused by altering the beam angle.) The stereo fields showed that, on a normal print, an apparently flat field of rods consisted of rods aligned at angles up to about 30° to the field and that the bundles or rods did not appear to have a definite reproducible cross section (e.g., square or round).

3.2.2. Gel Microsphere Cross Sections Prepared by a Microtome Technique

A praseodymium hydroxide gel microsphere (sol No. 95) was mounted in a standard methacrylate embedding medium, and ultrathin sections about 200 A thick were cut with a microtome. The sections were mounted on grids and examined at a magnification of 375,000 × (Fig. 7). A random distribution of rod-shaped crystals or thin sheets and bundles of rods or sheets was observed, with occasional square cross sections being noted where the orientation of the bundles allowed them to be cut at approximately 90° to the long axis. The width of the bundles varied from 30 to 150 A, and the maximum length was about 1000 A. The sharply defined bundle with an approximately square cross section near the bottom of Fig. 7 has a 140-A side and a mottled appearance, which suggests that there are several holes through the section. Many of the bundles are composed of parallel light and dark lines, each about 20 A wide, that are similar to the 30-A-wide lines observed on micrographs of β-FeO·OH.[8] The features in the micrographs may represent solid rods, or tubes, arranged parallel to each other, and/or thin sheets with one or more edges rolled up.

We have also obtained a thin section of a europium hydroxide gel sphere (No. 124), which showed (Fig. 8; magnification: 228,000 ×) a random distribution of bundles of rods or tubes similar to those shown in Fig. 7. However, the bundles were larger, about 240 to 380 A wide and up to 3000 A long. Cross sections of bundles cut approximately at right angles to the long axis were irregular, the majority having a "castellated" edge with a repeat distance of 75 to 80 A. These probably represent arrays of 4 × 4 or 3 × 3 units (rods or tubes). Several of the units or bundles of units showed curvature along the long axis, as was observed with β-FeO·OH crystals.[8] Micrographs of the sol No. 124 have been examined at magnifications of up to 658,000 × on the final prints. The prints (magnification: 501,000 ×) (see Fig. 9) showed patterns (arrows marked A) that can be

ORNL DWG 67-1580

Fig. 7. Microtomed Cross Sections of Pr Sol-Gel Beads.

ORNL DWG 67-1581

Fig. 8. Microtomed Cross Sections of Eu Sol-Gel Beads.

ORNL DWG 67-1582

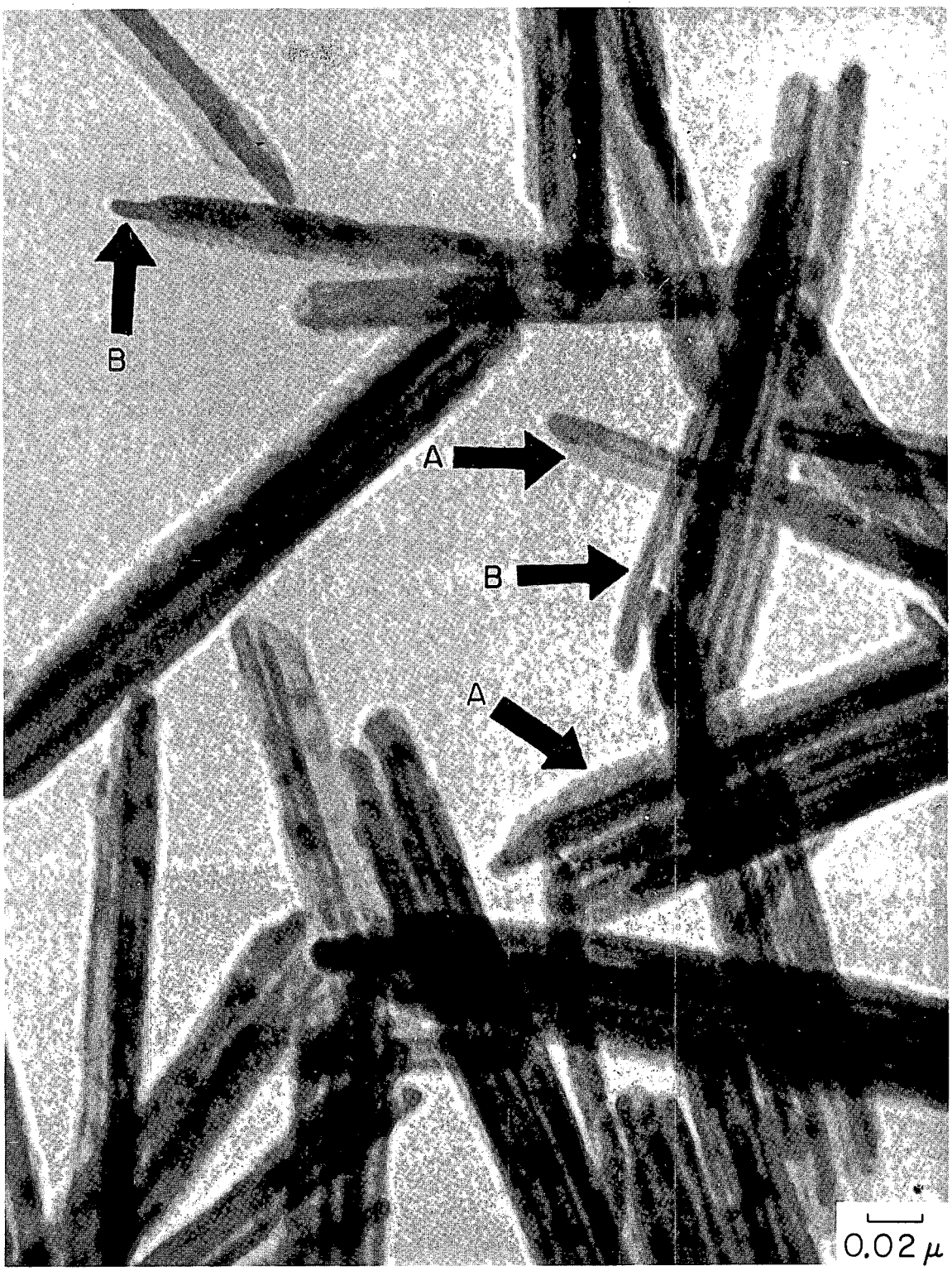

Fig. 9. Crystals of $Eu(OH)_3$ Showing Tube and Scroll-like Structure.

interpreted as thin sheets (15 to 20 A thick) with at least one rolled edge, as well as patterns (arrows marked B) that appear to arise from tubes (outside diameter, 60 to 70 A; inside diameter, 20 to 25 A). The patterns of overlapping light and dark lines in other areas are more difficult to interpret, but they may arise from bundles of tubes and rolled sheets.

3.2.3. Cross Section of Particles That Had Sedimented from a Sol

A europium hydroxide sol (No. 108) was allowed to stand in a tube at 25°C for several weeks, during which time a large proportion of the particles sedimented. The resulting layer of particles was dehydrated and embedded in plastic in a manner similar to that described by Watson.[8] A direct transmission electron micrograph of a section through a layer cut with a microtome is shown in Fig. 10. Bundles of rods cut both parallel and at right angles to the long axis can be seen. The length of the bundles is about 4000 to 5000 A, and the width or diameter of the bundles is 330 ± 50 A. Some of the bundles have a cross section that is approximately square, but nearly all have the castellated edges observed in the micrograph (Fig. 8) of the section through a europium hydroxide gel. The packing of the bundles is less uniform than that of the crystals in β-FeO·OH layers, in which a striking checkerboard pattern is seen (Fig. 2 of ref. 8).

3.2.4. Effect of Aging the Particles in the Mother Liquor

A comparison was made of the sizes and shapes of the particles in a precipitate of europium hydroxide (sol No. 138) (1) aged in the mother liquor (8 M NH_4OH, 0.1 M nitrate) for 24 hr, and (2) washed with water as in the normal sol preparation (Sect. 2.2) and aged in water at an apparent pH of 9.6 for 24 hr. Electron micrographs (Fig. 11) at a magnification of 165,000 × showed that (1) the particles in the mother liquor formed small plates about 300 A wide and that some of these were hexagonal with well-defined corners, (2) the particles aged in water were similar to those in Fig. 4C (bundles of rods or tubes 700 to 4000 A long and 60 to 300 A wide). A sample of the precipitate, which had been aged in the mother liquor for 24 hr, was then diluted by a factor of about 50 with water, and aged an additional hour; it showed some rod-shaped particles or rolled sheets, together with the small plates or sheets.

3.2.5. Conclusions About the Structure

The visual appearance of the micrographs of the washed and aged europium hydroxide sols and gels at high magnification was that of bundles of tubes and/or scrolls, each tube or rolled edge of a sheet having an outside diameter of about 60 to 70 A and an inside diameter of 20 to 25 A. However, in addition to groups of parallel lines, we observed single, dark lines about 20 A wide on the micrographs of the praseodymium hydroxide sols; hence solid, 20-A-diam rods (or small tubes) may coexist with large, 60-A-diam tubes. On aging, the rods or tubes grew longer, with those of praseodymium hydroxide (Fig. 3) and europium hydroxide (Fig. 4) reaching maximum lengths of 1000 and 7500 respectively; they did not appear to grow, first, as long sheets and then to roll up along the edges. The hydroxides of praseodymium and europium exhibited widely different rates of crystallization at 25°C, and the form of the crystals was influenced,

ORNL DWG 67-3617

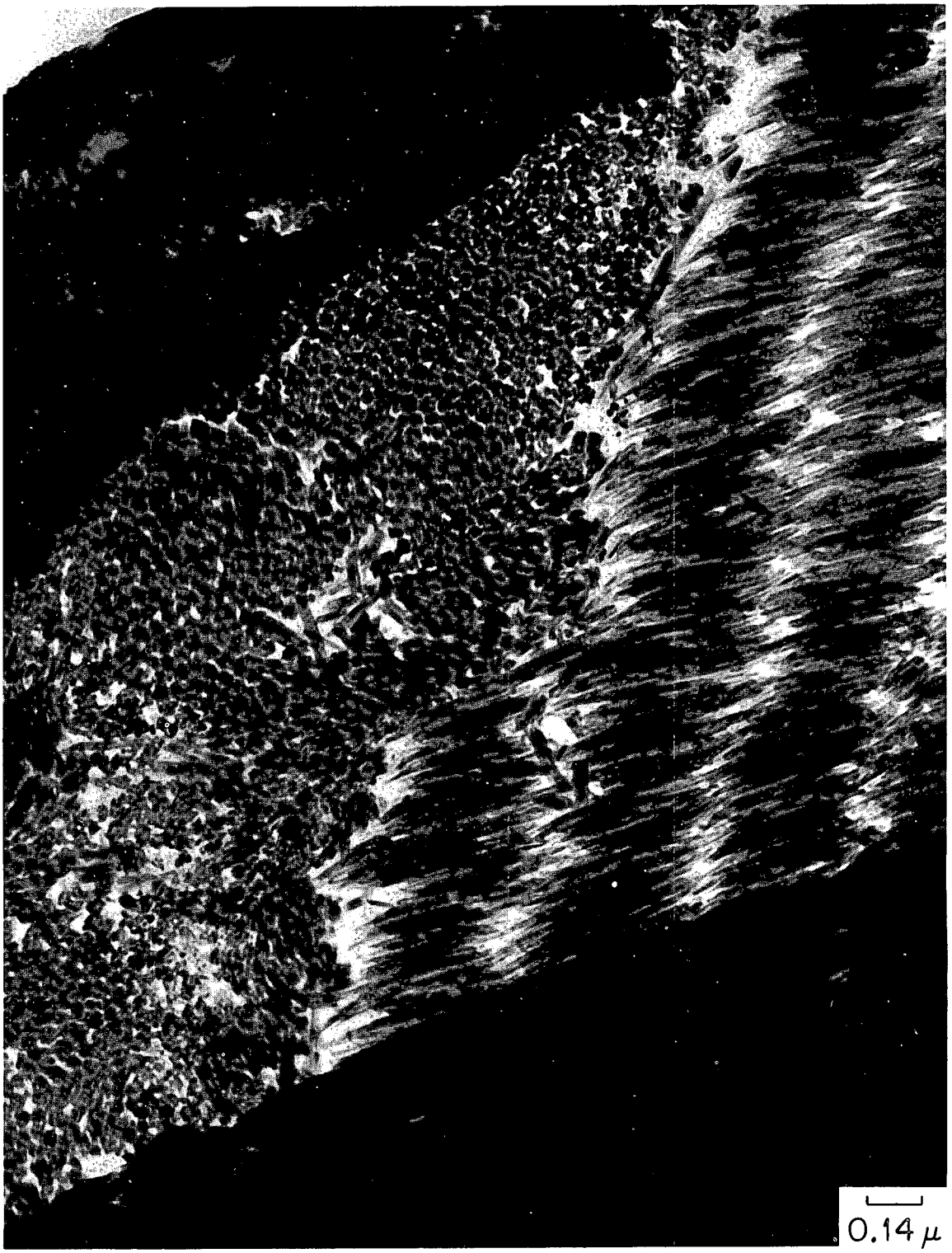

Fig. 10. Microtomed X-Section of Sedimented $Eu(OH)_3$ Sol.

ORNL DWG 67-3618

Fig. 11. $Eu(OH)_3$ Sol Aged in Mother Liquid for 24 hr.

to a large degree, by the nature of the solution in which the particles were aged [e.g., Fig. 4C (water) and Fig. 11 (8 M NH_4OH)].

It is possible that the crystal form in the sols could be controlled by preparing gel spheres with sheets or rods of such size that optimum properties (density, strength) would be produced in the final calcined oxide. Our efforts to modify the crystal form with additives are described below. In future work, scanning the electron micrographs with a recording microdensitometer may allow us to distinguish clearly between (1) parallel rods, (2) tubes, and (3) thin sheets with parallel, curled edges since a different density distribution with distance would be expected for each form.

3.3. Attempts to Change the Sizes and Shapes of the Particles

The random, loose packing of long bundles of rod-shaped particles in the gel microspheres (Fig. 7) leads to a degree of microporosity in the calcined oxide (see Sect. 6). If these particles were more closely packed, an oxide with a higher density and less porosity could probably be prepared. Therefore, we have made several attempts, all unsuccessful thus far, to change the sizes and shapes of the particles by (1) altering the temperature both during and after precipitation of the hydroxide, and (2) by adding formic acid as a complexing agent to prevent aggregation.

Praseodymium hydroxide was precipitated at 0°C and than aged at the same temperature for several hours (sol No. 97), while a sample of another sol (No. 93) was heated at 60°C for 4 hr. In both experiments, the electron micrographs showed that the sizes of the rods and bundles of rods were about the same (Table 9) as those obtained when the precipitate was formed and aged at 25°C (Table 8 and Fig. 3).

Formic acid was added at various stages in the preparation of the europium hydroxide sols Nos. 129, 130, and 131 (Table 4). After the precipitates for sols 129 and 130 had been thoroughly washed, formic acid was added to give formic acid/Eu mole ratios of 0.1 and 0.4 respectively; sufficient formic acid was added to sol 131 to give a formic acid/Eu mole ratio of 0.4 at the precipitation stage. Electron micrographs of the samples of the sols showed bundles of rods of about the same size as those observed for sols without formic acid. Thus it is probable that the formate ion forms only a weak complex with the europium ion, and that a reduction in the extent of aggregation will only be achieved with a very strong complexing ligand.

4. FORMATION OF MICROSPHERES

4.1. Formation of Gel Microspheres by Dehydration of Sols

Microspheres of gel were formed by injecting droplets of a sol into a long-chain alcohol or mixture of alcohols in (1) a baffled beaker whose contents was stirred at a rate just sufficient to keep the droplets suspended, and (2) a tapered column[9] in which an upflow of the alcohol fluidized the droplets. The alcohol partially dehydrated the sol spheres and allowed glossy spheres 20 to 200 μ in diameter to be formed in about 15

min in a beaker, or spheres 500 to 900 μ in diameter to be formed in 30 to 45 min in the column. These spheres were filtered from the solvent, washed with methanol, and dried; they were free-flowing at this stage. Although the tapered-column method required a longer period of dehydration (because of less turbulence), it had two advantages: (1) it produced spheres that were more uniform and of a more reproducible size than those obtained by the beaker method, and (2) the system could be operated continuously. One disadvantage noted was the tendency for the microspheres to agglomerate after a few minutes. This could be prevented only by adding a small amount (0.05 to 0.5 vol %) of a surface-active agent* (e.g., Amine-0, Span 80, Ethomeen S-15). In some instances, such additives caused the surfaces of the microspheres to be slightly irregular, and sols of different elements sometimes required different additives. For example, excellent glossy microspheres of praseodymium and neodymium hydroxide gels were formed in a column with 0.2% Amine-0 in 80% 2-ethyl-1-hexanol–20% 2-octanol, but europium hydroxide gels required a small amount (0.05 to 0.1%) of Span 80 in addition to Amine-0 to prevent agglomeration.

The size of the tapered column and the typical operating conditions in much of this work were:

Inside diameter at bottom, 10 mm
Inside diameter at top, 20 mm
Height of tapered section, 38 cm
Inside diameter of top settling section, 55 mm
Sol injection rate, 0.2 ml of 0.5 M sol per minute
Fluidizing rate, 100 ml/min (tangential input into 25-mm-diam section leading into a 10-mm narrow section)
Sol cut-off rate, 100 ml/min (past 20 gage hypodermic needle set at right angles to flow)
Residence time of spheres in column, 30 to 45 min
Average size of gel spheres under these conditions, 200 μ
Average output in an 8-hr day, 2.5 g of rare-earth oxide from 30 ml of 0.5 M sol

A larger-diameter column (four times the cross-sectional area and four times the internal capacity) was also operated with batches of about 30 ml of 0.5 M sols and 20 ml of 2 M sols, each batch requiring about a 2-hr operation. The production of 400- to 900-μ-diam spheres required the use of a relatively concentrated (e.g., 2 M) sol.

Photomicrographs of ~200-μ-diam microspheres of the hydroxide gels of cerium, praseodymium, and europium, together with the calcined oxide microspheres that are discussed in detail in Sect. 5, are shown in the color print (Fig. 12).

4.2. Formation of Gel Microspheres Directly from Nitrate Solution

The bulk of the nitrate and some of the water could be coextracted from droplets of a concentrated (2 to 3 M) solution of praseodymium

*Amino-0 (Geigy), cationic; Span 80 (Atlas), nonionic; Ethomeen S-15 (Armour), cationic.

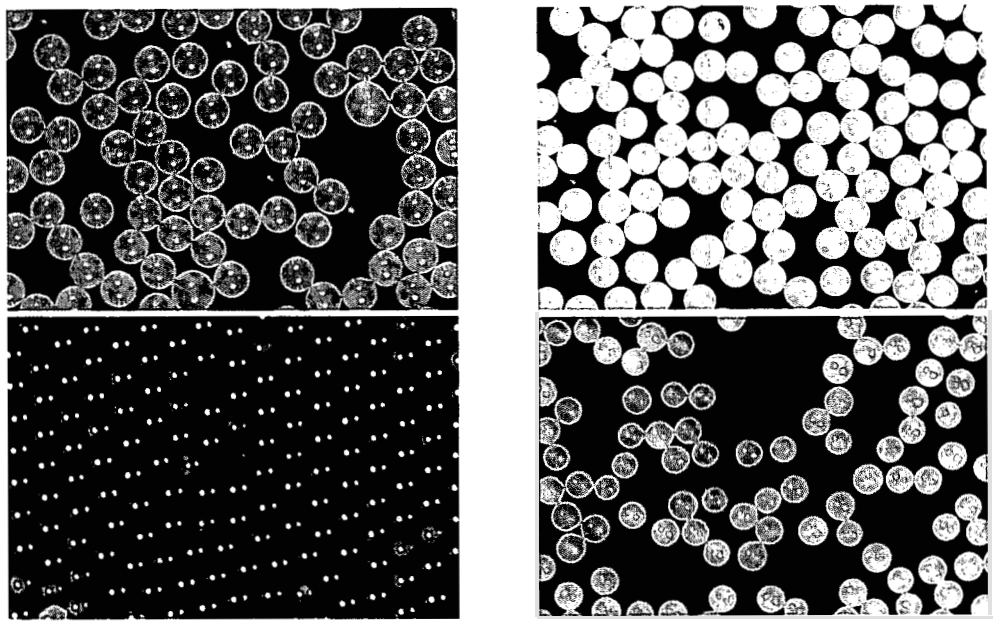

A B

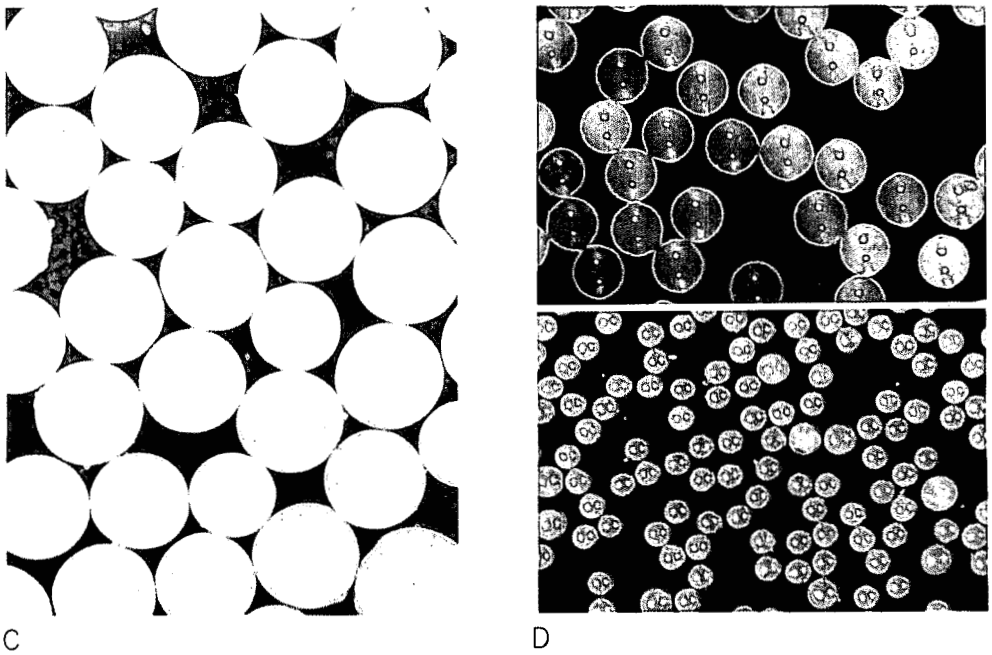

C D

A, top Praseodymium Hydroxide Gel, 195-215 μ Diam.
bottom Pr_6O_{11}, 1000°C, 135-155 μ Diam.

B, top Europium Hydroxide Gel, 170-200 μ Diam.
bottom Eu_2O_3, 1450°C, 100-125 μ Diam.

C, Sm_2O_3, 1200°C, 380-460 μ Diam.

D, top Cerium Hydroxide Gel, 180-190 μ Diam.
bottom CeO_2, 1000°C, 100-135 μ Diam.

Fig. 12. Photomicrographs of Microspheres of Lanthanide Hydroxide Gels and Lanthanide Oxides.

nitrate in water by combinations of a primary amine (Primene JMT), an alcohol (2-ethyl-1-hexanol), and an inert diluent (paraffin oil and diethylbenzene). Microspheres were formed by injecting the praseodymium nitrate solution from a hypodermic syringe into a beaker containing the solvent, which was stirred with a paddle stirrer. After the coextraction of nitrate and water for 15 to 30 min, the spheres were removed by filtration or centrifugation, washed with methanol, air-dried, and sized with standard sieves.

The effects of varying the relative amounts of amine, alcohol, and diluent on the extent of nitrate removal and on the size and appearance of the microspheres were studied. The preferred method, in terms of a low-nitrate content and good shape of the spheres, was to denitrate and dehydrate with 20 to 25 vol % amine (no alcohol) in a diluent having a viscosity and a density that serve to keep the droplets suspended and to maintain the required size. Combinations of a viscous paraffin oil and diethylbenzene were used in order that a range of viscosities could be studied. A highly viscous mixture gave very small, perfect, glassy spheres, whereas a low-viscosity mixture gave spheres that were larger but with a less perfect shape and with more surface irregularities. Batches that had good spherical particles with a glassy or translucent appearance were dried at 100°C and calcined at 1000 to 1200°C.

Praseodymium oxide-hydroxide microspheres 5 to 10 μ in diameter were prepared; however, it was not possible to measure their resistance to crushing forces because they were too small to be mounted in the instrument that was available. After these microspheres were calcined in air at 1200°C for 3 hr (5 hr required to reach 1200°C), x-ray line-broadening measurements on batch 21 indicated that the crystallite sizes ranged from 580 to 610 A, and that the cubic phase of $PrO_{1.83}$ was present (a = 5.47 A).

The effect of temperature on this system was also examined. Denitration of droplets of praseodymium nitrate solution (~2 M) with 5% Primene JMT in 20% ethylbenzene/75% paraffin oil diluent at 80 to 90°C gave NO_3^-/Pr mole ratios of about 1, compared with ratios of 0.3 to 0.4 at 25°C; hence the higher temperature did not give lower nitrate contents as it did with thorium nitrate.[10] Several small batches of europium hydroxide gel microspheres were made at 50 to 90°C; the higher temperatures gave microspheres of a larger size (up to 100 μ in diameter), but probably with higher nitrate contents (by analogy with the results for praseodymium). A small proportion of the microspheres had a good shape, high surface gloss, and a bluish, translucent appearance, but the bulk of the product consisted of broken or whole shells.

In summary, the main difficulties that were experienced were:

(1) Removal of the nitrate. The lowest NO_3^-/Pr mole ratio achieved was 0.3, which may be too high to obtain strong, dense spheres, according to our previous experience with products from the precipitation method of producing sols of praseodymium hydroxide.
(2) Control of the sphere size. Spheres 10 to 30 μ in diameter, as well as a few batches of a larger size were produced, but 100- to 200-μ-diam spheres of good shape and appearance were difficult to obtain.
(3) Control of drying rate. If the droplets were dried too rapidly, the product spheres were broken and consisted of small crystals (rather than a glass); the spheres crushed easily both before and after calcination. Further experiments are planned to optimize the conditions and to obtain a lower nitrate content.

5. CALCINATION OF GEL MICROSPHERES TO OXIDE MICROSPHERES

5.1 Method of Calcination

Gel microspheres were converted to oxide microspheres by:

(1) drying them at 100 to 120°C for several hours;
(2) heating them to 500°C at a rate of 50 to 100°C/hr, and holding them at that temperature for several hours to decompose residual nitrate; and
(3) heating them from 500 to between 1000 and 1500°C at a rate of 50 to 100°C/hr, and holding them at the desired maximum temperature for 2 to 5 hr to achieve a high-density oxide.

Photomicrographs of calcined microspheres of the oxides of Ce, Pr, Eu, and Sm are shown in the color print (Fig. 12); the physical properties of these and other similar products are discussed in Sect. 6. The amount of shrinkage that occurred in the various stages for the gel sphere to

Table 11. Shrinkage of Microspheres in Calcination of Gel to Final Oxide

Stage	Conditions			Mean Diameter[a] of Spheres (μ)	Shrinkage Factor[b]
	Time (hr)	Temperature (°C)	Atmosphere		
			Crystalline Europium Hydroxide Gel[c]		
A	16	25	Vacuum	558	1
B	2	125	Vacuum	558	1
C	3	500	Vacuum	526	1.06
D	3	900	Vacuum	490	1.14
E	3	1400-1450	Air	330[d]	1.69[d]
			Amorphous Europium Hydroxide Gel[e]		
A'		25		198	1
B'		1000		106[d]	1.87[d]
C'	3	1450		93[d]	2.13[d]

[a] Diameters of 30 spheres formed from the crystalline gel and 50 spheres formed from the amorphous gel were measured with a binocular microscope with calibrated eyepiece scale.

[b] Based on diameter measurements.

[c] From 3 M sol No. 138.

[d] Crush resistance and crystal form for sol No. 147 and for preparations similar to sol No. 138 are given in Table 14.

[e] From 0.5 M sol No. 147.

the final oxide sphere is shown in Table 11 for gel spheres prepared from:

(1) a concentrated (3 M) sol (No. 138) of crystalline europium hydroxide (most of the shrinkage occurred in the range 900 to 1450°C);
(2) a dilute (0.5 M) sol (No. 147) of amorphous europium hydroxide (most of the shrinkage occurred in the range 25 to 1000°C).

Electron micrographs and x-ray data for the spheres at the various stages are presented in Sect. 6.2.

The gel spheres were heated up to 1000°C, usually in vacuum, to prevent absorption of carbon dioxide from the air and also to assist in the removal of traces of organic material (e.g., 2-ethyl-1-hexanol and surface-active agents) that was not very volatile. Since it was thought that the presence of small amounts of nitrate and carbonate at relatively high temperatures might lead to a lower resistance to crushing and a lower density in the final oxide spheres, the thermal decomposition of lanthanide nitrates and carbonates was examined by infrared spectroscopy (Sec. 5.2).

5.2. Decomposition of Nitrates and Carbonates of Lanthanide Elements

The gel microspheres produced from hydroxide sols contain nitrate remaining from, or added during, the sol-gel procedure, and sometimes contain carbonate as an impurity. Infrared spectra of gels and of hydrated nitrates and carbonates of Pr, Nd, and Eu, and of samples of these materials heated to various temperatures up to 1500°C, were measured to assist in the interpretation of the mode of their decomposition. The spectra showed that the nitrate was decomposed during the presoaking step at 500°C (prior to heating to 1500°C in the normal calcination method) but that carbonate was decomposed only if the sample was heated for several hours at 900°C.

The changes in the spectra of the nitrates of Pr and Eu with temperature suggested that a considerable change had occurred in the bonding of the residual nitrate groups to the metal atoms at temperatures above about 300°C. Thermogravimetric analyses[11,12] indicated that extensive decomposition of the lanthanide nitrates had taken place above this temperature; the weight changes were interpreted as evidence of the presence of stable compounds of the anhydrous trinitrate of Pr from 300 to 425°C,[11] and a basic nitrate of Eu from 450 to 500°C.[12]

Spectra of europium nitrate (1) crystallized from solution at 50°C, (2) heated for 2 hr at 300°C, and (3) heated for 2 hr at 400°C are shown in Fig. 13. The absorption bands at 1486, 1283, 1040, 1024, 810, and 749 cm^{-1} were typical[13] of the nitrato group coordinated to a metal atom; there was no evidence for the presence of the nitrate ion.

New bands were obtained at temperatures greater than 300°C, at 1602, 1197, 820, and 713 cm^{-1} (the band at 1602 cm^{-1} arises from nitrate instead of water because there is no associated water band at about 3400 cm^{-1}). These bands do not correspond to those recently reported[14] for the anhydrous nitrate of Eu. It has been suggested by Vratny[15] that bands observed at about these frequencies in the decomposition of praseodymium nitrate arise from nitrite, and in particular, from nitrite in a bridging configuration.

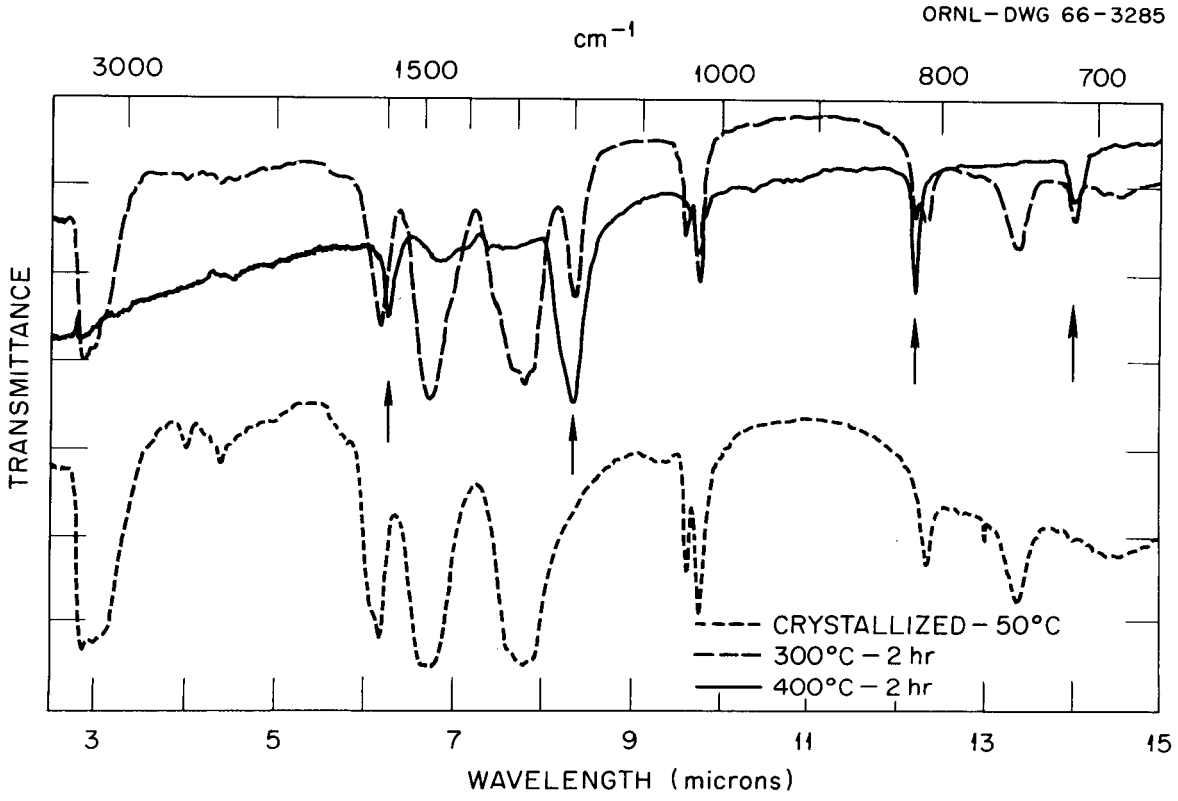

Fig. 13. Infrared Spectra of Europium Nitrate.

Therefore, we prepared samples of praseodymium nitrite and europium nitrite by two methods and measured their infrared spectra. The first method consisted in adding a solution of silver nitrite to a solution of lanthanide chloride, filtering the precipitated silver chloride, and evaporating the filtrate to dryness. The second method involved fractional crystallization from mixed solutions of lanthanide nitrate and silver nitrite. The spectra of the lanthanide nitrites showed no contaminating nitrate or silver nitrite and were different from the spectrum that was reported by Vratny for praseodymium nitrite.

The new bands in the spectra at 400°C (Fig. 13) were located at frequencies similar to those which were observed for anhydrous nitrato complexes of various metals and which were postulated as being attributable to bridging or bidentate bonding of the nitrate groups to the metal.[13] Thus, we suggest that these lanthanide nitrates decompose through an intermediate bidenate (or bridging) nitrate structure, rather than through a bridging nitrite structure.

The bands in the europium carbonate spectra changed considerably when the sample was heated to temperatures above about 300°C. The bands in the spectra of a sample that was dried for 18 hr at 75° (Fig. 14) were at 1500, 1380, 1060, and 856 cm^{-1}, and were typical of carbonate groups coordinated to metal atoms.[13] A number of sharp bands (e.g., at 3050, 2800, 2440, 1760, 1720, 878, 702 cm^{-1}) appeared when the sample was

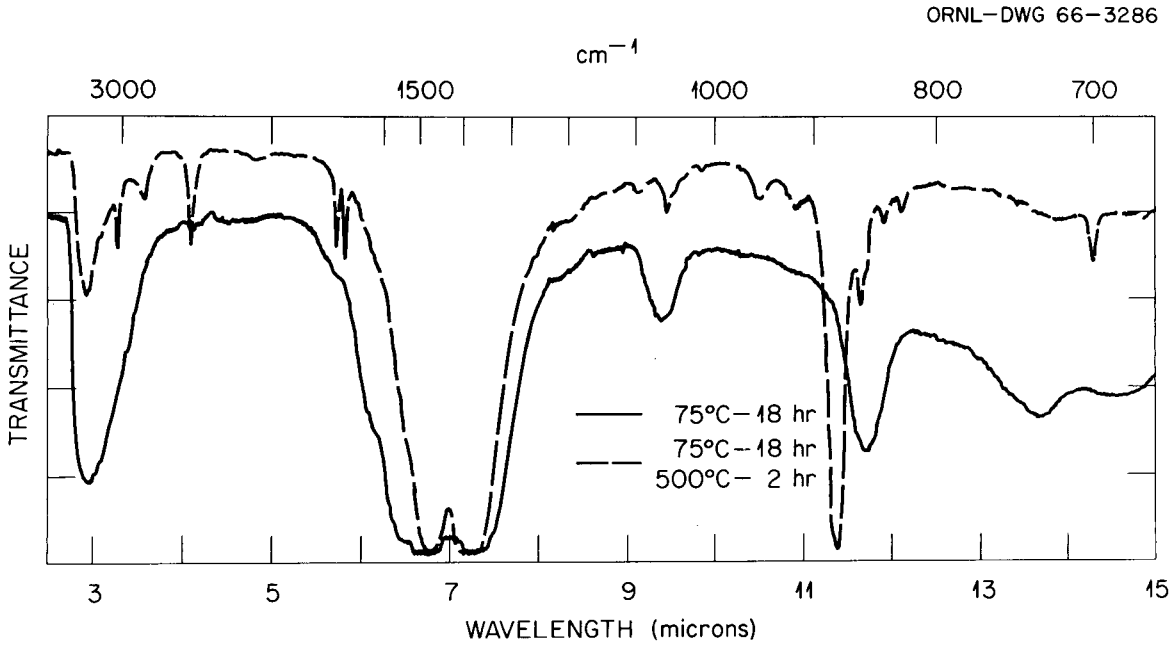

Fig. 14. Infrared Spectra of Europium Carbonate Heated to 75° and 500°C.

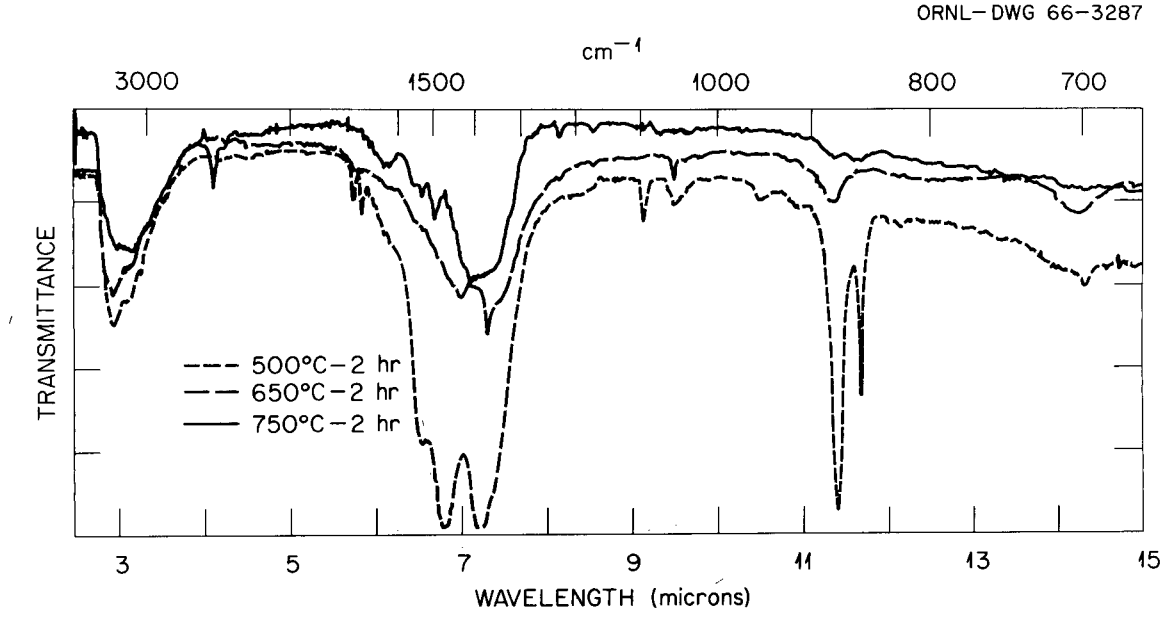

Fig. 15. Infrared Spectra of Europium Carbonate Heated to 500, 650, 750°C.

further heated to 500°C for 2 hr (Fig. 14). The bands at high frequencies were probably overtone and combination bands, but the lower ones were fundamentals of the carbonate group and were shifted with respect to those in the sample dried at 75°C. When the sample was heated to 750°C for

2 hr (Fig. 15), the two strong bands at about 1500 and 1400 cm^{-1} decreased considerably in intensity (principally because of decomposition) and merged into one broad band centered on 1390 cm^{-1}. The band assigned to the symmetrical C-O stretching vibration at 1060 cm^{-1} (Fig. 14) disappeared in the samples heated to temperatures higher than 650°C, and the bands remaining were more like those of the carbonate ion than of the coordinated carbonate group.[16]

Decomposition of the last trace of carbonate was accomplished only by heating the sample to 900°C for several hours. Thus, in the calcination of metal hydroxide gel microspheres, carbonate, when present in a significant amount, will be decomposed only in the final sintering stage (at 900 to 1400°C). The presence of carbonate in this final stage can affect the density and the crush resistance of the product.

6. PHYSICAL PROPERTIES AND STRUCTURE OF LANTHANIDE OXIDE MICROSPHERES

6.1. Physical Properties

The density, surface area, crystal form, crystallite size (by x-ray line-broadening), and crush resistance were determined for samples of microspheres of lanthanide oxides that were prepared by the calcination of gel microspheres (Tables 12 and 13).

The crush resistance of the microspheres was measured in an apparatus that consisted of a flat tungsten carbide plate fixed to a screw supported rigidly above a flat tungsten carbide plate on the pan of a laboratory rough balance. Each sphere was placed between the parallel flat plates, and the weight was increased gradually by adding water to a 1-liter measuring cylinder on the opposite pan of the balance. A microphone was attached to the top tungsten carbide plate and was coupled to an amplifier and loudspeaker; a loud "pop" indicated that the sphere had been crushed. This method gives a useful comparison between batches of spheres prepared under different conditions, but may not be useful as an absolute method.

The crush resistances of microspheres of Pr_6O_{11} and Eu_2O_3 were measured as a function of the particle diameters (Fig. 16). Groups of ten particles having diameters ranging from 90 to 360 μ were selected by using a binocular microscope fitted with an eyepiece scale (the diameter values used are averages of ten determinations, the maximum deviation from the mean being about ± 40%). The praseodymium hydroxide sol was prepared as described in Sect. 2.1 and was formed into microspheres of gel in a beaker. The europium hydroxide sols were prepared as described in Sect. 2.2 and formed into microspheres in a column. Since sol No. 147 was not heated, the colloidal particles were amorphous and the Eu concentration was 0.45 M. On the other hand, sol Nos. 140, 144, and 145 were heated for 1 hr at 80°C to form crystalline colloidal particles and were concentrated to 2.5 to 3 M in Eu before the gel spheres were formed. The strength of the monoclinic Eu_2O_3 spheres (Fig. 16) that were heated to 1450°C increased with the 1.5 power of the diameter over the range 90 to 200 μ, whereas the strength of both the cubic Eu_2O_3 spheres that were heated to 1000°C and the Pr_6O_{11} spheres increased as the square of the diameter.

Table 12. Physical Data for Lanthanide Oxide Microspheres Prepared by the First Method[a]

Oxide of Metal	Sol No.	Precipitant Used	Conditions of Calcination[b]		Density[c]		Surface Area (m^2/g)	Crystal Form	Crystallite Size[d] (A)	Crush Resistance[e] (g)
			Temperature (°C)	Time (hr)	g/cc	% of Theoretical				
Pr	52	TMAH	120-180 1050	1 22.5				$PrO_{1.83}$ cubic		375
Eu	73-1	TMAH	250 Fast to 1200 1480	60 2.5	8.11	100	0.033	Monoclinic	500	330
Eu	73-2	TMAH	120-175 Slow to 500 Fast to 1500	2 0.5 3	7.65	95.7	0.016	Monoclinic	600	322
Eu	75	NH_4OH	25 Slow to 500 Fast to 1500	15 0.5 3	7.62	95.2	0.009	Monoclinic	600	220
Eu	76	NH_4OH	Same as for sol No. 75		7.51	94.2	0.011	Monoclinic		216
Eu	78	TMAH	Same as for sol No. 75		7.79	97.2	0.014	Monoclinic	600	
Eu	79	TMAH	Same as for sol No. 75		7.62	95.2	0.008	Monoclinic	550	286
Eu	80	NH_4OH	Same as for sol No. 75		7.75	97.2	0.010	Monoclinic	600	252
Eu	81	TMAH	Same as for sol No. 75		7.81	97.7	0.153	Monoclinic	750	<100

[a]See Sect. 2.1.
[b]In air.
[c]By toluene method.
[d]By x-ray line broadening.
[e]Average of ten spheres 150 μ in diameter.

Europium oxide microspheres were usually calcined at a final temperature of 1400 to 1500°C to obtain the monoclinic form, which was thought to be more satisfactory than the cubic form for fabrication into cermets with stainless steel or aluminum.[17] The monoclinic form has a theoretical crystal density of 7.99 g/cc and the following lattice dimensions:[2] a, 14.082 A; b, 3.604 A; c, 8.778 A; β, 100° 00.[1] The bcc form that is obtained at 1000°C has a theoretical crystal density of 7.28 g/cc and a lattice dimension of 10.87 A.[2] The cubic form can be converted into the monoclinic form slowly at 1050°C or in 2 hr at 1400°C; this change is not easily reversible.[18]

The observation of a large difference in strength between microspheres of cubic Eu_2O_3 that had been formed at 1000°C from amorphous gel spheres and microspheres of monoclinic Eu_2O_3 that had been formed at 1450°C from crystalline gel spheres led to a more detailed examination of crush resistance as a function of the crystallinity of the gel spheres and the temperature of calcination. The results are summarized in Table 14, from which the general conclusions are:

1. The strongest oxide spheres were obtained as the cubic form (density, 94% of theoretical; strength, 600 g for 150-μ-diam spheres) by heating amorphous gel spheres to 1000°C; these spheres usually had a glassy internal appearance and a rough external surface.

2. Monoclinic oxide spheres obtained by heating the amorphous gel spheres directly to 1450°C were appreciably weaker (229 g); those obtained by heating the gel spheres to 1000°C followed by cooling and reheating to 1450°C were weaker still (120 g).

Table 13. Physical Data for Lanthanide Oxide Microspheres Prepared by the Second Method[a]

Oxide of Metal	Sol No.	Conditions[b] of Calcination		Density[d]		Surface Area (m^2/g)	Crystal Form	Crystallite Size[f] (A)	Resistance[g] to Crushing (g)
		Temperature (°C)	Time (hr)	g/cc	% of Theoretical				
Eu	101B	120	4				Monoclinic	400	268
		500	1				Eu_2O_3		
		1450	3						
Nd	104	Slow to 900[c]					Hexagonal	600	280[h]
		1200	3				Nd_2O_3		
Pr	105	50[c]	3				Cubic	200 (220 plane)	613
		500[c]	4				$PrO_{1.83}$	350 (111 plane)	
		1000[c]	4.5						
Eu	106	50-100[c]	4				Monoclinic	600	252
		1000[c]	2				Eu_2O_3		
		1450	3						
Eu	107	Slow to 500[c]	1				Monoclinic	630	310[i]
		1450	3				Eu_2O_3		
Eu	108	(1)Slow to 950[c]	2				Cubic	630-750	~70
							Eu_2O_3		
		(2)As above; then		7.35	92	0.071	Monoclinic		192
		1450	3				Eu_2O_3		
Ho	111	(1)Slow to 500[c]					Ho_2O_3		215[h]
		1475	3						
		(2)Fast to 1450	3				Ho_2O_3		142
Eu	115	(a)Slow to 500[c]					Monoclinic		156[h]
		1475	3				Eu_2O_3		
		(b)Fast to 1475	3				Monoclinic		172[h]
							Eu_2O_3		
Eu	118	Slow to 500	0.5	7.43	93	0.024	Monoclinic	625	
		750[c]	1.5				Eu_2O_3		
		1475	3.5						
Eu	119	125[c]	72	7.50	94		Monoclinic		
		Slow to 900[c]	4				Eu_2O_3		
		1475	3						
Eu	124	Fast to 500[c]	1	7.62	95		Monoclinic	650	
		1475	3				Eu_2O_3		
Eu	127	25[c]	60				Monoclinic		
		Slow to 500[c]	1	7.82	98.2		Eu_2O_3		
		1475	3						
Nd	133	Slow to 500[c]	1	7.20[e]	97.5		Hexagonal		1400[j]
		1100	2				Nd_2O_3		
Sm	134A	Slow to 500[c]	1	7.34	95		Monoclinic		1600-2500[j]
		1200	3				Sm_2O_3		
	134B	As 134A; then					Monoclinic		650[k]
		1600	2				Sm_2O_3		

[a]See Sect. 2.2.
[b]Calcination was done in air except where stated.
[c]Calcination done in vacuum.
[d]By toluene method
[e]Density by helium method.
[f]By x-ray line broadening.
[g]Values are averages of measurements made on ten 150-μ-diam spheres.
[h]Based on 120-μ-diam spheres converted to 150-μ-diam spheres by 1.5 power law.
[i]Based on 105-μ-diam spheres converted to 150-μ-diam spheres by 1.5 power law.
[j]Measurements made on 450-μ-diam spheres.
[k]Measurements made on 390-μ-diam spheres.

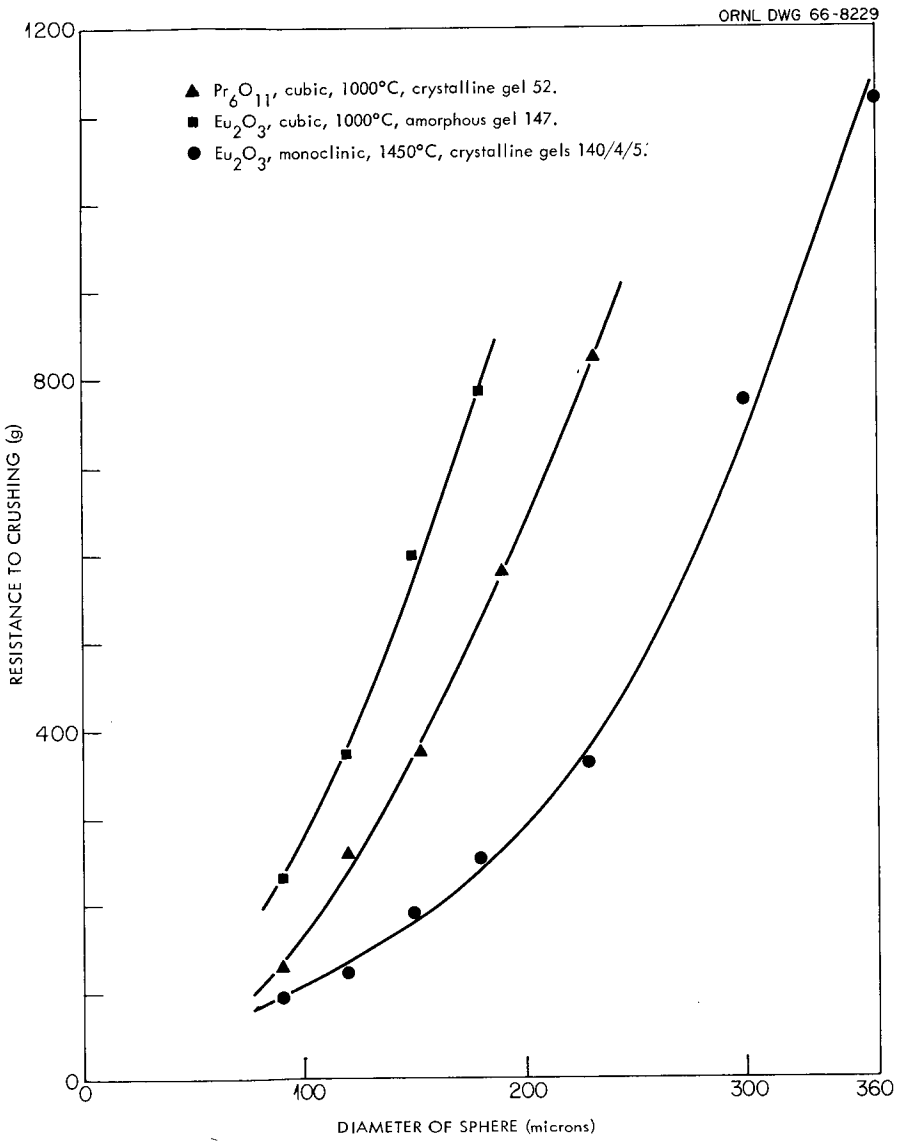

Fig. 16. Crushing Strengths of Eu_2O_3 and Pr_6O_{11} as a Function of Microsphere Diam.

3. Oxide spheres prepared in the cubic form at 1000°C from crystalline gel spheres had no appreciable strength (<50 g), and many samples showed plastic deformation compared with the brittle fracture observed for spheres that were heated to a higher temperature or were made from amorphous gel spheres.

4. The average strength of monoclinic Eu_2O_3 spheres prepared at 1450°C from crystalline gel spheres was 190 g, that is, of the same order as that observed in monoclinic Eu_2O_3 spheres prepared from amorphous gel spheres; hence the transformation of the cubic to the monoclinic structure is probably the main factor in the decreased strength above about 1000°C.

5. The strength of cubic Eu_2O_3 spheres calcined at 1000°C from freshly prepared amorphous gel spheres was about the same as that for spheres made from gel spheres that had been aged for four months at 25°C.

Table 14. Effects of the Structure of the Gel Spheres and the Temperature of Calcination on the Crush Resistance of Eu_2O_3 Microspheres

Structure of Colloidal Particles in Gel	Age of Gel	Code No.	Temperature of Calcination (°C)	Structure of Oxide	Crush Resistance of 150-μ-diam Spheres (g)
Amorphous	1-2 days	147	1000	Cubic	600[a]
Amorphous	1-2 days	147	1000; reheated 1450° for 3 hr	Monoclinic	175
Amorphous	4 months	119	1000	Cubic	590
Amorphous	4 months	119	Heated directly to 1450 for 3 hr	Monoclinic	229
Amorphous	4 months	119	1000; reheated to 1450 for 3 hr	Monoclinic	120
Crystalline	1-2 days (heated 1 hr at 80°)	Several preparations	1000	Cubic	<50
Crystalline	1-2 days (heated 1 hr at 80°)	Several preparations	1000; reheated to 1450 for 3 hr	Monoclinic	190[b]

[a]Density, 6.84 g/cc; 94% of theoretical value.
[b]Density, 7.58 g/cc; 95% of theoretical value.

Electron microscopy and electron diffraction patterns of the aged gel spheres (batch No. 119, Table 14) showed that the colloidal particles were either amorphous or only poorly crystalline and about 300 A in diameter, compared with the large rod-shaped crystals (up to 7000 A long) in typical crystalline gel spheres. The gel state, therefore, appeared to hinder crystallization of the particles over a period of four months at 25°C, whereas large crystalline particles are formed in less than 24 hr at 25°C in liquid sols of europium hydroxide.

From the standpoint of the practical use of europium oxide microspheres in control rods in reactors, or in other applications, there is a choice of two products:

(1) Cubic Eu_2O_3 microspheres that are calcined at 1000°C and have a density of about 95% of theoretical, a crush resistance of about 600 g for 150-μ-diam spheres, and a range of diameters from 50 to 200 μ.

(2) Monoclinic Eu_2O_3 microspheres that are calcined at about 1400°C and have a density of about 95% of theoretical, a crush resistance of about 200 g for 150-μ-diam spheres, and a range of diameters from 50 to 500 μ (the range is greater because the crystalline sols can be concentrated to 2 to 3 M in Eu, thus allowing larger spheres to be formed; in contrast, the more viscous, amorphous sols cannot be concentrated easily). The size distribution of a batch of 35 g of monoclinic Eu_2O_3 spheres from three combined batches, which were designed to have diameters ranging from 90 to 150 μ, is given in Table 15; 77 and 88% of the batch had diameters in the ranges 88 to 149 μ and 88 to 177 μ respectively.

Samples of Nd_2O_3 and Sm_2O_3 were heated to 1200 and 1600°C, and the crystal structures (and resistances to crushing) were examined to determine whether the high-temperature hexagonal form was produced. Results showed that the Nd_2O_3 was in the hexagonal form at both 1200 and 1600°C but that Sm_2O_3 was in the monoclinic form. We observed that the Nd_2O_3 microspheres were unstable toward uptake of water vapor and disintegrated in a few hours if exposed to the laboratory air; they were stable if kept in a sealed tube. Microspheres of cubic Pr_6O_{11}, monoclinic Sm_2O_3, and monoclinic Eu_2O_3 were

Table 15. Size Distribution of Eu_2O_3 Microspheres[a] in a 35-g Batch Prepared from Sols Nos. 140, 144, and 145

Sieve Size (μ)	Weight (g)	Percentage of Total Batch Weight
>210	0.204	0.58
210-177	0.943	2.67
177-149	4.244	12.02
149-125	7.460	21.13
125-105	12.573	36.60
105-88	6.723	19.04
<88	3.175	8.99

[a]Crush resistance is shown as a function of diameter in Fig. 16. Density is 95% of theoretical crystal density.

stable in air. The Sm_2O_3 spheres calcined at 1600°C were much less resistant to crushing than those calcined at 1200°C (Table 13). The instability of the hexagonal form of these oxides has been reported previously[19] and is one reason why this form is not used in the ceramic industry.

The carbon content of the final calcined oxides was low, for example, 0.004 wt % in Eu_2O_3 microspheres prepared from sol No. 118, and 0.002 wt % in Eu_2O_3 microspheres prepared from sol No. 128.

6.2. Structure

The external and internal structures of the oxide microspheres were examined (1) by optical microscopy of the as-received spheres and of spheres polished by standard metallographic techniques (using alumina and diamond abrasives in silicon oil instead of water to prevent hydration) and (2) by electron microscopy of replicas of as-received surfaces, etched polished surfaces, and fracture surfaces.

Polished cross sections of 80- to 120-μ-diam microspheres of cubic Pr_6O_{11} (sol No. 105) and monoclinic Eu_2O_3 (sol No. 106) are shown in Fig. 17. In sample 106 we observed a large number of small, closed pores, which were probably the result of too low a concentration of metal (e.g., 0.5 M) at the time of gel sphere formation. Sols of Pr (No. 123) and Eu (No. 124) were concentrated in a rotary film evaporator to about 2 M in metal and were subsequently formed into gel microspheres that showed less porosity after calcination. Cross sections of about 400-μ-diam microspheres of Nd_2O_3 (hexagonal, 1200°C, sol No. 133) and Sm_2O_3 (monoclinic, 1200°C, sol No. 134) are shown in Fig. 18. These had no significant porosity and had densities that were 97.5 and 95% of the theoretical crystal densities respectively.

Electron micrographs of replicas of the external surface of a monoclinic Eu_2O_3 sphere (sol No. 138 heated to 1450°C) showed (see Fig. 19) grains about 2 to 7 μ wide and irregular boundaries. A pronounced stepped surface was observed on many of the grains, the smallest step heights being about 200 A. This carbon replica, and the following ones, were prepared with an initial plastic film (Faxfilm) that was shadowed with Pt-C, coated with carbon, and the plastic film removed.

Electron micrographs of replicas of the polished internal surface of metallographic specimens (e.g., similar to those in Figs. 17 and 18) revealed no detailed structure. However, when the polished surface was etched for a few seconds in 8 M HNO_3, replicas showed considerable structural detail as follows:

(1) Oriented arrays of crystals within each grain. One such array is shown in Fig. 20 for an Eu_2O_3 sphere (monoclinic, 1450°, from sol No. 124). Adjacent grains (e.g., Fig. 21) showed different appearances as a result of different crystal faces being exposed and being dissolved at different rates. The end faces of the crystals in the grain in Fig. 20 were 1000 to 3000 A wide, and the flat crystal faces in adjacent grains (e.g., Fig. 21) were 2000 to 8000 A wide.
(2) Circular or elliptical closed pores about 2000 A wide. These were probably pores in the original material, rather than gas bubbles formed on the surface during the etching procedure.

PHOTO 83245

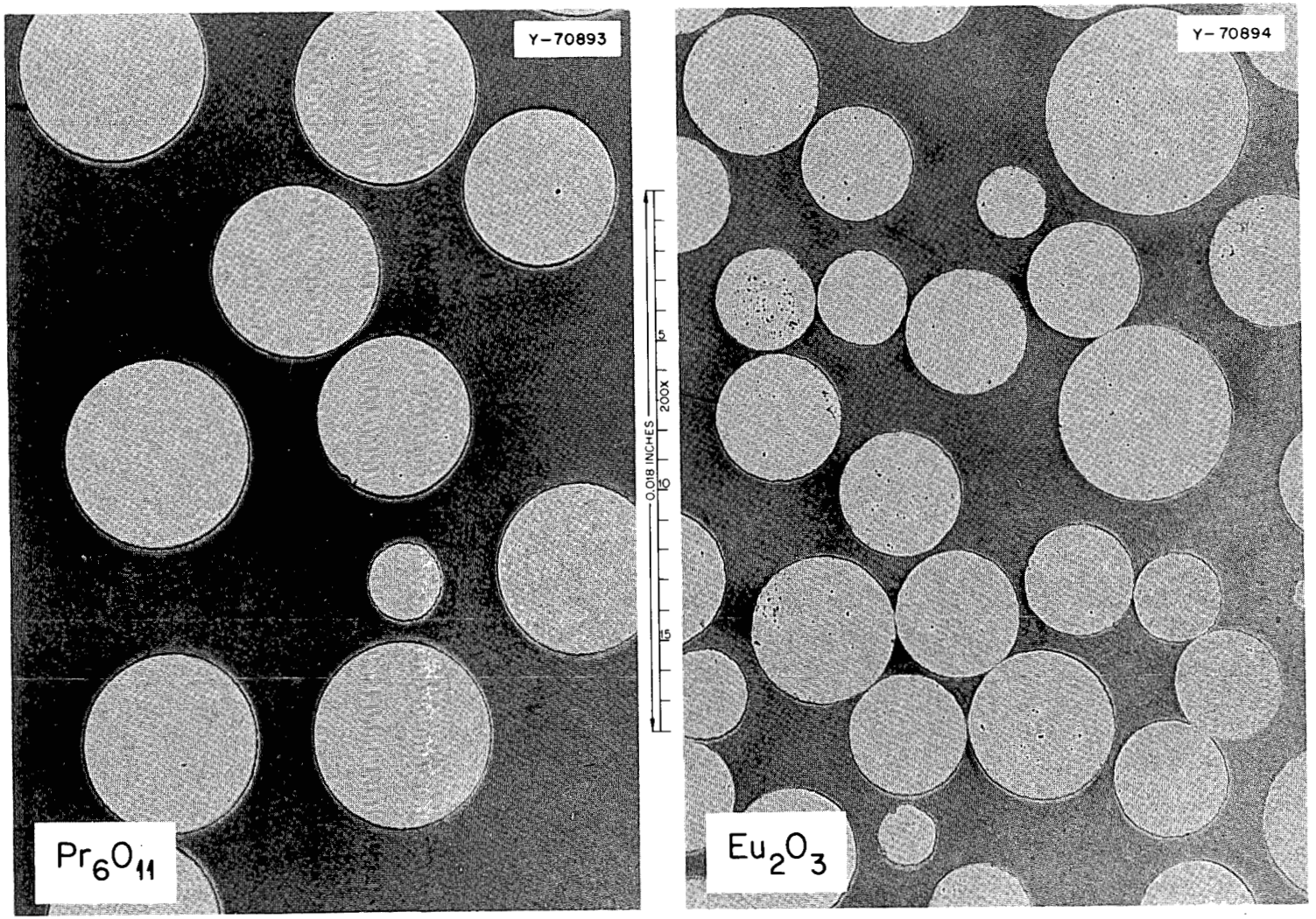

Fig. 17. Polished Cross-Sections of Microspheres of Pr_6O_{11} and Eu_2O_3.

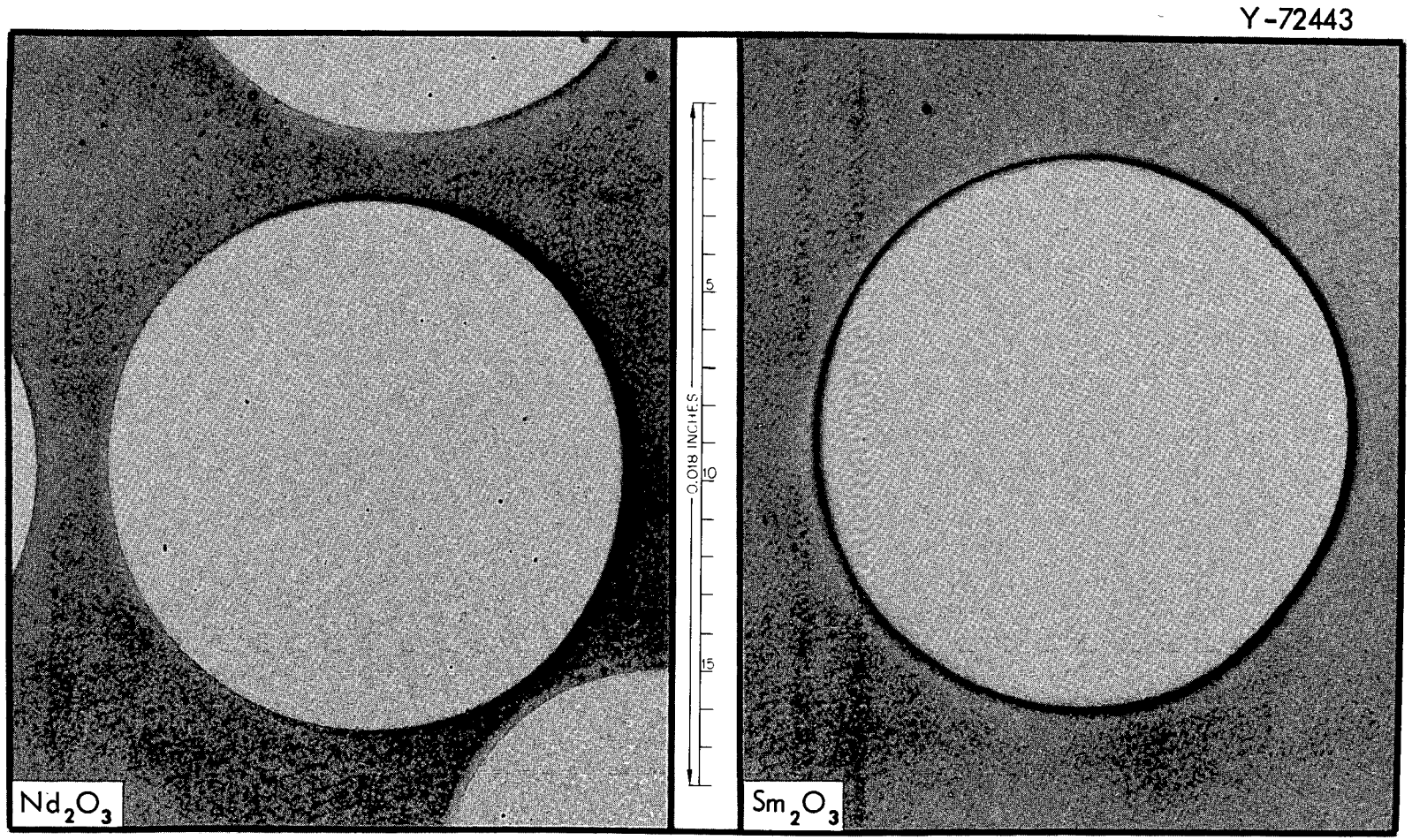

Fig. 18. Polished Cross-Sections of Microspheres of Nd_2O_3 and Sm_2O_3.

ORNL DWG 67-3619

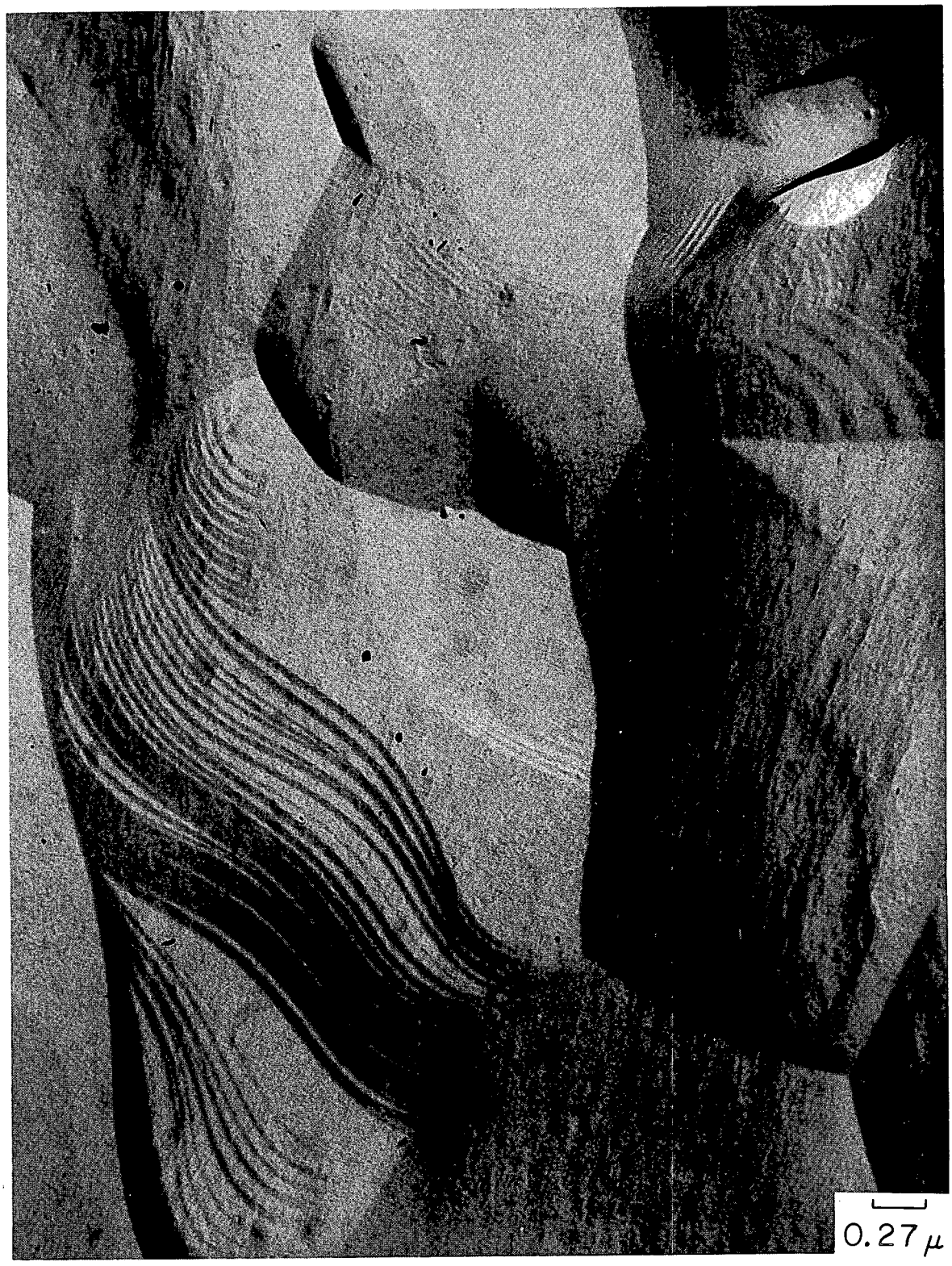

Fig. 19. External Surface of Eu_2O_3 Microsphere Calcined at 1400-1450°C for 3 hr.

ORNL DWG 67-3620

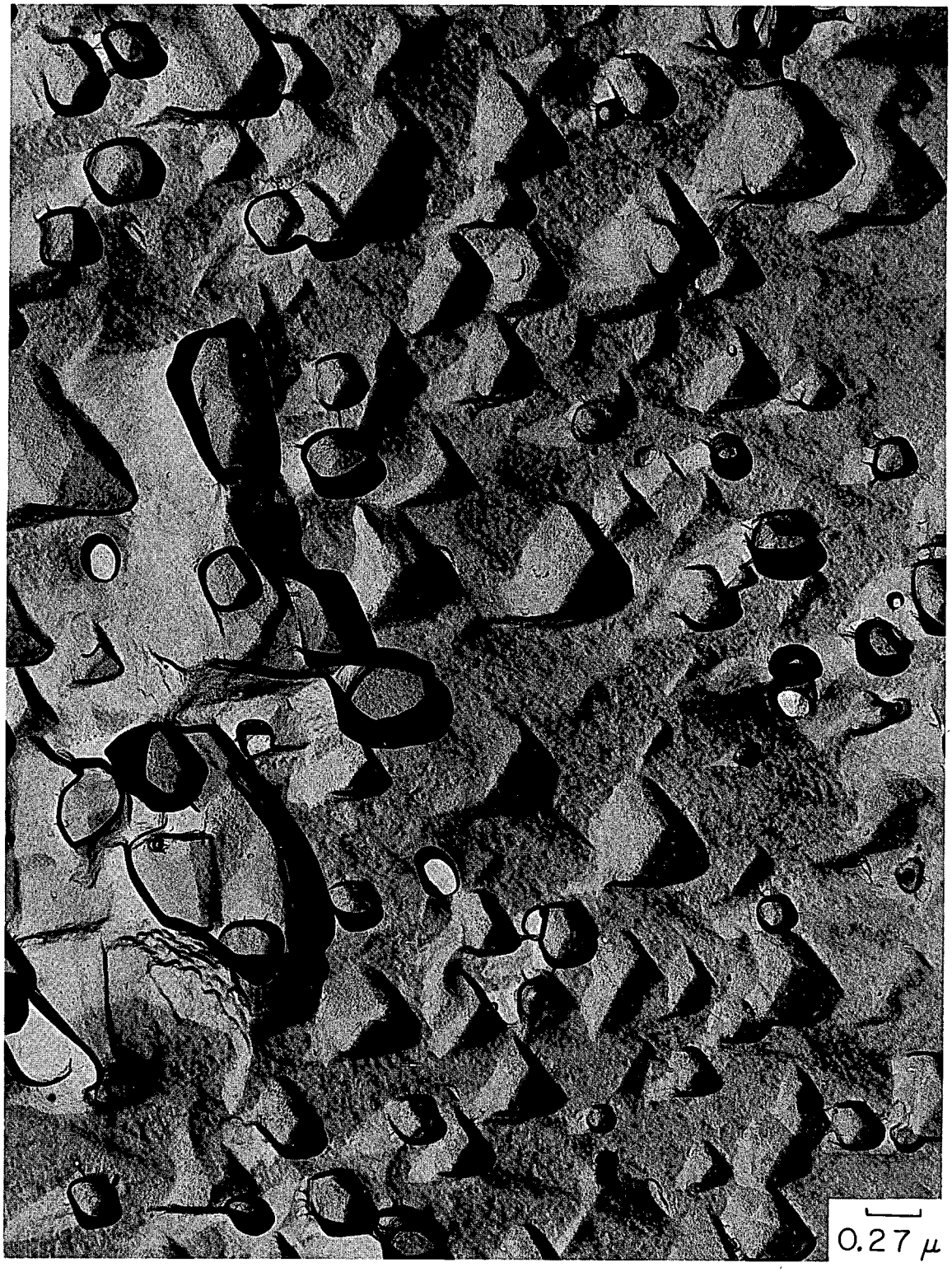

Fig. 20. Polished and Etched Cross Section of Eu_2O_3 Microspheres Calcined at 1400-1450°C for 3 hr Showing the End Faces of Crystals.

ORNL DWG 67-3621

Fig. 21. Polished and Etched Cross Section of Eu_2O_3 Microspheres Calcined at 1400-1450°C for 3 hr Showing the Flat Crystal Faces.

An electron micrograph of a replica of a fracture surface of an Eu_2O_3 sphere (monoclinic, 1450°, from sol No. 124) is shown in Fig. 22. This (and many other fractographs) shows the presence of grains with irregular boundaries but does not show the detailed structure within the grains; it also shows pores on the fracture surface having apparent diameters of up to 5000 A. One fractograph showed a grain in which there was a large degree of twinning.

Electron micrographs of the internal structure of microspheres at the various stages in the calcination procedure are shown in Figs. 23 to 26 (see also Table 11 for data on shrinkage of the spheres). The europium hydroxide gel spheres (sol No. 138) dried at 25 and 125°C in vacuum were sectioned with a microtome, but those that were calcined at higher temperatures were too brittle to cut with a microtome; hence Pt-C-shadowed replicas of fractured surfaces were obtained. The main features of the figures and related x-ray data are summarized in Table 16.

7. APPLICATIONS

By using the methods outlined in this report, we can prepare lanthanide oxides in the form of dense oxide microspheres of controlled size (or irregularly shaped aggregate if required) without the use of a high-temperature furnace or an arc-fusion method, and without excessive wastage or sieving operations. In principal, these methods are also applicable to the preparation of sols, gels, and oxides of the transplutonium elements, of which americium and curium (as dense oxides) are of interest for incorporation into targets for irradiation in the High Flux Isotope Reactor at Oak Ridge (to produce transcurium isotopes).

Currently, lanthanide oxides are used only to a small extent in industry; however, they will undoubtedly become more important in the future.[20] Some potential applications of individual oxides are:

(1) incorporation of samarium, gadolinium, or europium oxides in cermets in reactor control rods, or as burnable poisons in fuel elements;

(2) use of europium or thulium oxides (containing highly radioactive Eu or Tm isotopes, e.g., ^{152}Eu, $t_{1/2}$ = 13 years; ^{171}Tm, $t_{1/2}$ = 1.9 years) as a radioactive heat source for an artificial heart pump that is now being studied by the U.S. Department of Health;[21]

(3) use of oxides of promethium isotopes ^{147}Pm, ($t_{1/2}$ = 2.5 years) as intense beta-ray sources;

(4) production of metal oxide catalysts containing lanthanide oxides[22] in a very fine state of division by mixing a sol of a lanthanide hydroxide with a suitable sol of a compound of another element and calcining the mixture (this method may also be applicable to making lanthanide oxide phosphors[23] with a uniform distribution of the activating ions in the host lattice).

ORNL DWG 67-3622

Fig. 22. Fractured Surface of Eu_2O_3 Microsphere Calcined at 1400-1450°C for 3 hr.

ORNL DWG 67-3623

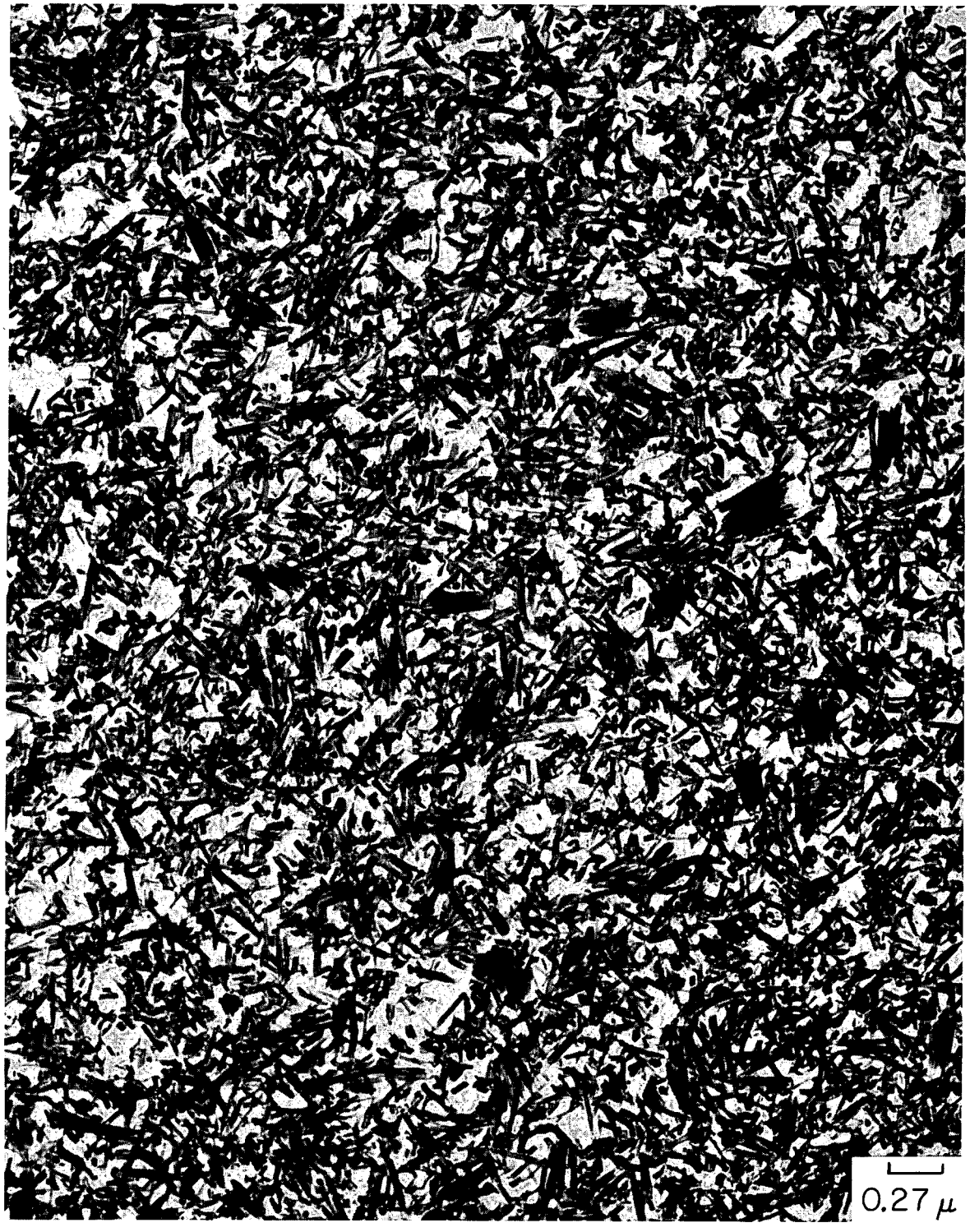

Fig. 23. $Eu(OH)_3$ Sol Washed and Aged at 25°C for 16 hr.

ORNL DWG 67-3624

Fig. 24. Fractured Surface of $Eu(OH)_3$ Microsphere Showing the Beginning of Conversion to Eu_2O_3 (cubic).

ORNL DWG 67-3625

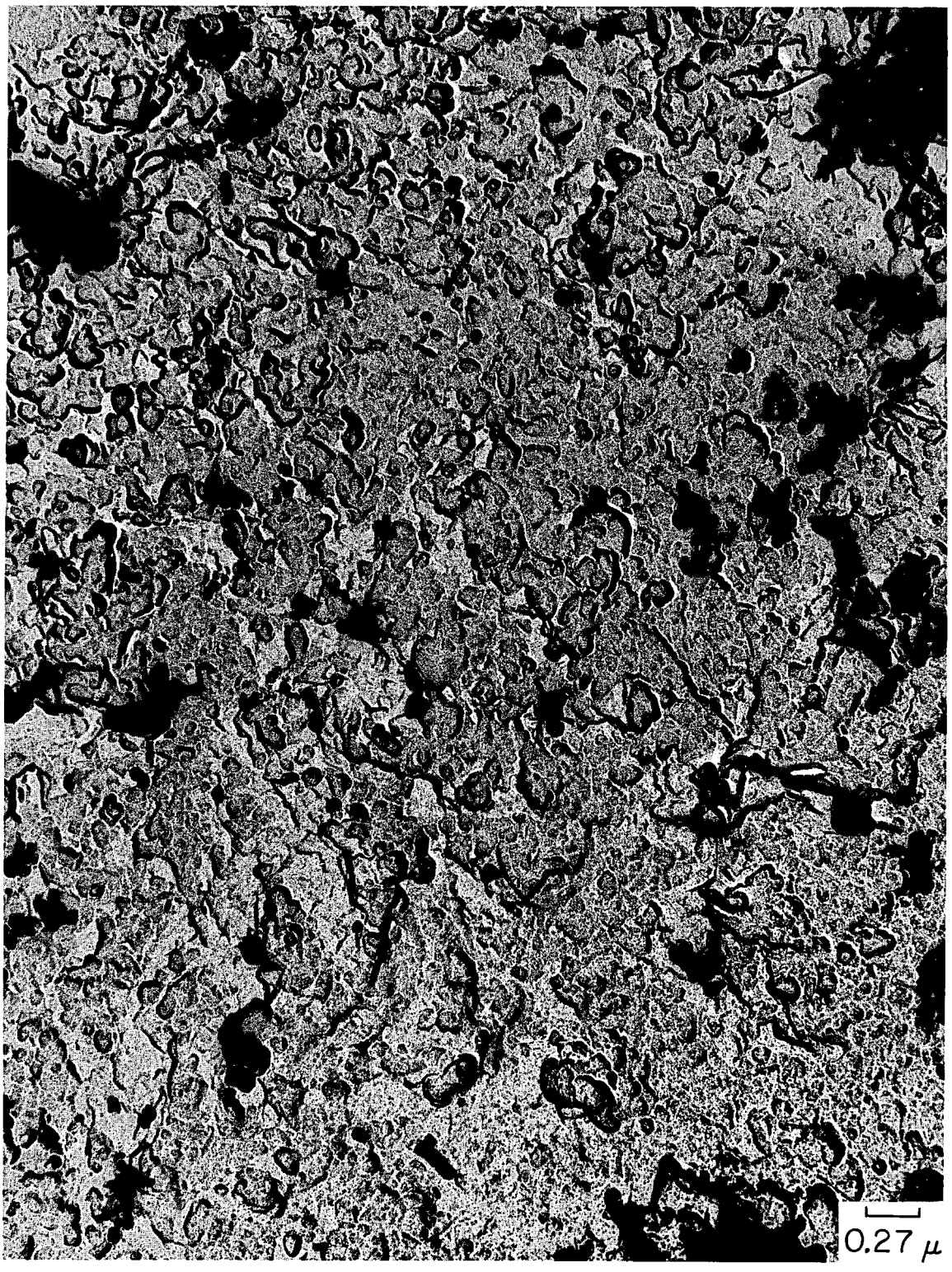

Fig. 25. Fractured Surface of Eu_2O_3 (cubic) Calcined at 900°C for 3 hr.

ORNL DWG 67-3626

Fig. 26. Fractured Surface of Eu_2O_3 Microsphere Calcined at 1400-1450°C for 3 hr.

Table 16. Internal Structure of Microspheres at Various Stages in the Calcination of Europium Hydroxide Gel (No. 138) to Monoclinic Europium Oxide

Fig. No.	Conditions of Calcination				Structural Features from Micrographs	X-Ray Data
	Stage	Time (hr)	Temperature (°C)	Atmosphere		
23	A	16	25	Vacuum	Random array of bundles of crystalline rods of $Eu(OH)_3$; large void space probably filled with water	
Not illustrated	B	2	125	Vacuum	Similar to A	
24	C	3	500	Vacuum	Generally featureless background with superimposed black[a] areas	Cubic Eu_2O_3 and hexagonal $Eu(OH)_3$; 200-A crystallites
25	D	3	900	Vacuum	Closely packed small grains with superimposed black areas which are probably a hydroxide relic structure	Cubic Eu_2O_3; 360-A crystallites
26[b]	E	3	1450	Air	Large, flat grains (1-5 μ) with pronounced step structure; also, dome-shaped crystals with small flat facets	Monoclinic Eu_2O_3; 500-A crystallites

[a]The dense black areas are the result of small crystals adhering to the first plastic replica and then to the carbon replica when the plastic was stripped from the carbon.

[b]See also Fig. 19 for typical external surface of these spheres.

ACKNOWLEDGMENTS

Gratitude is expressed to members of the Analytical Chemistry Division for determining densities, surface areas, and trace impurities; R. G. Sherman for obtaining x-ray data; T. E. Willmarth for photomicrographs, electron micrographs, and electron diffraction data; the Metallography Section of the Metals and Ceramics Division for polished cross sections and photomicrographs; B. Weaver, C. F. Leitten, R. D. Baybarz, and O. L. Keller for supplying lanthanide compounds; F. J. Smith for measuring the charge on sol particles; D. O. Campbell, J. P. Young, and J. T. Bell for assistance with the use of Cary model 14 spectrophotometers; and O. L. Keller and G. Begun for assistance with the Cary Raman spectrometer.

R. E. Leuze and R. G. Wymer are thanked for helpful discussions throughout the course of the work.

REFERENCES

1. W. O. Milligan and David W. Dwight, J. Electronmicroscopy (Tokyo) 14, 264 (1965).

2. R. C. Rau, p. 117 in Rare-Earth Research II, Proceedings of the Third Conference on Rare-Earth Research, April, 1963, Clearwater, Fla., ed. by K. S. Vorres, Gordon and Breach, New York, 1964.

3. R. W. G. Wyckoff, Crystal Structures, 2d ed. Interscience, New York, 1963.

4. C. K. Jorgenson, Matemat-fys. Med. Kon. Danske Videns. Sels. 30, No. 22 (1956).

5. G. Oster, Chem. Rev. 43, 319 (1948).

6. B. D. Chun, Properties of Colloidal Thoria (Thesis), University of Utah, 1964.

7. R. Roy and H. A. McKinstry, Acta Crist. 6, 365 (1953).

8. J. H. Watson, R. R. Cardell, and W. Heller, J. Phys. Chem. 66, 1757 (1962).

9. J. P. McBride, ORNL-3874 (1966).

10. J. G. Moore, private communication, 1965.

11. W. W. Wendlandt, Anal. Chim. Acta 15, 435 (1956).

12. W. W. Wendlandt and J. L. Bear, J. Inorg. Nucl. Chem. 12, 276 (1960).

13. B. O. Field and C. J. Hardy, Quart. Rev. (London) 18, 383 (1964).

14. A. Walker and J. R. Ferraro, J. Chem. Phys. 43, 2689 (1965).

15. F. Vratny, Trans. Faraday Soc. 56, 1051 (1960).

16. B. M. Gatehouse, S. E. Livingstone, and R. S. Nyholm, J. Chem. Soc. (London), 3137 (1958).

17. C. F. Leitten, ORNL-2733 (1959); ORNL-2422 (1957).

18. C. E. Curtis and A. G. Tharp, J. Am. Ceram. Soc., 42, 151 (1959).

19. M. W. Shafer and R. Roy, J. Am. Ceram. Soc., 42, 563 (1959).

20. F. H. Spedding and A. H. Daane, p. 522 in The Rare-Earths, sect. IV, Wiley, New York, 1961.

21. Nucleonics Week, 6 (No. 23), 5 (1965).

22. A. A. Tolstopyatova and A. A. Balandin, p. 333 in Rare-Earth Elements, Academy of Sciences, U.S.S.R., 1959; National Science Foundation, Washington D.C. (translation); and references therein.

23. R. C. Ropp, p. 481 in Rare-Earth Research II, Proceedings of Third Conference on Rare-Earth Research, April, 1963, Clearwater, Fla., ed. by K. S. Vorres, Gordon and Breach, New York, 1964.

ORNL-4000
UC-25 — Metals, Ceramics, and Materials

INTERNAL DISTRIBUTION

1. Biology Library
2-4. Central Research Library
5-6. ORNL — Y-12 Technical Library
Document Reference Section
7-26. Laboratory Records Department
27. Laboratory Records, ORNL R.C.
28. G. M. Adamson
29. R. D. Baybarz
30. R. J. Beaver
31. J. E. Bigelow
32. R. E. Biggers
33. R. E. Blanco
34. W. D. Bond
35. G. E. Boyd
36. R. B. Briggs
37. R. E. Brooksbank
38. K. B. Brown
39. F. R. Bruce
40. S. R. Buxton
41. J. M. Chandler
42. Ji Young Chang
43. S. D. Clinton
44. C. F. Coleman
45. D. J. Crouse
46. F. L. Culler
47. J. E. Cunningham
48. D. E. Ferguson
49. L. M. Ferris
50. B. R. Fish
51. J. H Frye, Jr.
52. H. E. Goeller
53. A. T. Gresky
54. P. A. Haas
55-65. C. J. Hardy
66. R. G. Haire
67. F. E. Harrington
68. C. C. Haws, Jr.
69. M. R. Hill
70. J. D. Hoeschele
71. A. R. Irvine
72. F. A. Kappelmann
73. O. L. Keller
74. M. T. Kelley
75. E. E. Ketchen
76. H. T. Kite
77. C. E. Larson
78-82. R. E. Leuze
83. M. H. Lloyd
84. H. G. MacPherson
85. M. M. Martin
86. W. R. Martin
87. J. P. McBride
88. K. H. McCorkle
89. A. B. Meservey
90. J. G. Moore
91. J. P. Moore
92. L. E. Morse
93. E. L. Nicholson
94. K. J. Notz
95. R. B. Parker
96. W. L. Pattison
97. J. T. Roberts
98. A. D. Ryon
99. R. L. Sherman
100. M. J. Skinner
101. J. W. Snider
102. R. E. Thoma
103. W. E. Unger
104. J. E. Van Cleve
105. B. S. Weaver
106. A. M. Weinberg
107. M. E. Whatley
108. J. C. White
109. T. E. Willmarth
110. M. K. Wilkinson
111-115. R. G. Wymer
116. P. H. Emmett (consultant)
117. J. J. Katz (consultant)
118. E. A. Mason (consultant)
119. C. W. J. Wende (consultant)

EXTERNAL DISTRIBUTION

120. J. A. Swartout, Union Carbide Corporation, New York, N.Y.
121. M. E. Wadsworth, University of Utah, Salt Lake City, Utah
122. Jake Glatter, Bettis Atomic Power Laboratory, P.O. Box 1468, Pittsburgh, Pennsylvania
123. B. L. Vondra, NUMEC, Apolla, Pennsylvania
124. Kermit Alexander, Knolls Atomic Power Laboratory, Schenectady, New York
125. W. Wild, Director Atomic Energy Research Establishment, Harwell, England
126. M. E. A. Hermans, N.V. KEMA, Utrechtseweg 310, Arnhem, Netherlands
127-128. J. M. Fletcher, Atomic Energy Research Establishment, Harwell, England
129. Th. von der Plas, N.V. KEMA, Afd, K.R.L., Utrechtseweg 310, Arnhem, Netherlands
130. R. G. Sowden, UKAEA Liaison Office, British Embassy, Washington, D.C.
131. Richard Proelstle, Knolls Atomic Power Laboratory, Schenectady, New York
132. Research and Development Division, AEC, ORO
133-404. Given distribution as shown in TID-4500 under Metals, Ceramics, and Materials category (25 copies — CFSTI)